U.S. DEPARTMENT OF
ENERGY

Office of
ENERGY EFFICIENCY &
RENEWABLE ENERGY

Accelerated Stress Testing of Multi-Source LED Products: Round 2

July 2019

(This page intentionally left blank)

RTI Project Number
0215939.001.001

Accelerated Stress Testing of Multi-Source LED Products: Round 2

July 2019

Prepared for

U.S. Department of Energy

Through contract with
KeyLogic Systems, Inc.
3610 Collins Ferry Road
Morgantown, WV 26505

Prepared by

RTI Authors: Lynn Davis, Kelley Rountree, Michelle McCombs, and Karmann Mills
RTI International
3040 E. Cornwallis Road
Research Triangle Park, NC 27709

Acknowledgments

The material in the report is based upon work supported by the U.S. Department of Energy's Office of Energy Efficiency and Renewable Energy (EERE), under award number DE-FE0025912.

Disclaimer

This report was prepared as an account of work sponsored by an agency of the United States Government. Neither the United States Government nor any agency thereof, nor any of their employees, makes any warranty, express or implied, or assumes any legal liability or responsibility for the accuracy, completeness, or usefulness of any information, apparatus, product, or process disclosed, or represents that its use would not infringe privately owned rights. Reference herein to any specific commercial product, process, or service by trade name, trademark, manufacturer, or otherwise does not necessarily constitute or imply its endorsement, recommendation, or favoring by the United States Government or any agency thereof. The views and opinions of authors expressed herein do not necessarily state or reflect those of the United States Government or any agency thereof.

Nomenclature or List of Acronyms

°C	degree Celsius
%T	transmittance
$\Delta u'$	change in the u' chromaticity coordinate
$\Delta u'v'$	magnitude of chromaticity shift
$\Delta v'$	change in the v' chromaticity coordinate
AST	accelerated stress testing
CCT	correlated color temperature
CIE	International Commission on Illumination (*Commission Internationale de l'Eclairage*)
CSM	chromaticity shift mode
CTL	color-tunable lighting
Cu-Sn	copper–tin
CW	cool white
DUT	device under test
DW	Durbin–Watson statistic
e	natural logarithm base
EMI	electromagnetic interference
hr, hrs	hour, hours
HP-LED	high-power light emitting diode
IES	Illuminating Engineering Society
K	Kelvin
L	lower asymptotic limits
L_{70}	the time at which the light output from the lamp is 70% of the initial luminous flux
LED	light-emitting diode
mA	milliAmp
MOSFET	metal–oxide–semiconductor field-effect transistor
MP-LED	mid-power light emitting diode
NIR	near infrared
NIST	National Institute of Standards and Technology
nm	nanometer
p	wavelength

PAR	parabolic aluminized reflector
PC	polycarbonate
PCB	printed circuit board
pcLED	phosphor-converted light-emitting diode
PCT	polycyclohexylenedimethylene terephthalate
PMMA	polymethyl methacrylate
p_o	peak wavelength
PPA	polyphthalamide
R	average reflectance
R^2	R squared (correlation coefficient)
R_{70}	radiant flux at 70% of its initial value
R_o	initial average reflectance in the visible range
SPD	spectral power distribution
SSE	sum of squared error
SSL	solid-state lighting
t	time
UV-Vis	ultraviolet visible absorption
V	volt
W	watt
WTL	white-tunable lighting
WW	warm white
YAG:Ce	cerium-doped yttrium aluminum garnet

Executive Summary

The benefits of solid-state lighting (SSL) products that use light-emitting diodes (LEDs) over conventional lighting products are numerous and include energy savings, longer lifetimes, and a greater ability to adjust the spectral output of the device. Spectral adjustment is desired in applications in which multiple lighting spectra are required, and some examples of locations that might use adjustable spectrum lighting include hospitals, offices, nursing homes, classrooms, and greenhouses. Although LED sources with fixed correlated color temperatures (CCTs) can provide good optimization in some of these settings, greater control over the spectral content is often gained by using multi-source LED products. The reliability of LED modules with multiple LED sources is not well understood; therefore, this report, which is second in a series of reports about multi-source LED lighting products, focuses on determining the mechanisms of optical change in multi-source LED products that use different types of mid-power LEDs (MP-LEDs) integrated into the same LED module. The earlier report (Round 1)[1] in this series provided initial accelerated stress testing (AST) results for the products studied in this current report, and future reports will benchmark advancements from other devices.

The products studied in this report provide spectral tuning and use different LED primaries consisting of different types of LEDs in MP-LED packages to provide spectral adjustments. The specific devices under test (DUTs) examined in this report include a white-tunable light (WTL) product (referred to as MULTI-TW1) and two horticulture growth lamps (referred to as MULTI-H1 and MULTI-H2). The Multi-TW1 LED module is intended for indoor use in offices and classrooms to promote good working and learning environments, and it consists of 40 warm white and 40 cool white MP-LEDs (both are phosphor-converted LEDs [pcLEDs] with a blue pump but different phosphors). The two horticulture lamps, MULTI-H1 and MULTI-H2, optimize the red-to-blue radiant power ratios to assist plant growth, but they do so with two different architectures for the LED module that capitalize on the advantages of different MP-LED packages. The MULTI-H1 horticulture lamp contains an LED module consisting of a single type of pcLEDs made with a blue pump and red phosphor, whereas MULTI-H2 horticulture lamp contains an LED module consisting of two different types of MP-LED packages: a group of 6 pcLEDs (with a blue pump and broad green phosphor) and a group of 10 direct-emitting red LEDs.

This report summarizes the overall findings from up to 20,000 hrs of AST on the Multi-WT1 LED module DUTs and up to 8,000 hrs of AST on the horticulture lamp DUTs. During the ASTs described herein, the population of MULTI-WT1 DUTs was subjected to a power cycling test in elevated ambient temperatures of either 75°C or 95°C, with each temperature population being further subdivided into four testing currents. The DUT populations of the two horticulture lamp products were subjected to a power cycling test in a temperature and humidity environment of 65°C and 90% relative humidity (6590). Details are provided regarding the causes of chromaticity and radiant flux changes and the impacts that these changes have on the ability of the DUTs to maintain the application-specific lighting spectrum marketed to the consumer. The key findings of this report cover the relative impacts of the LEDs, including the LED chip, phosphors, and packages; secondary device optics (e.g., lenses, reflectors); and device electronics on the long-term reliability of the multi-source LED products. Because of the characteristics of multi-source LED products, the impacts of these system components upon product reliability may be different from that of single-source LED products and may represent new challenges in reliability engineering that must be identified, and then characterized to obtain an understanding of the lifetime performance of these new lighting technologies.

The reliability of the LEDs in each DUT's LED modules had a significant impact on the long-term chromaticity and radiant flux reliability of the multi-source LED products. It was found in this report and an

[1] Davis, J. L., Rountree, K. J., & Mills, K. C. (2018). *Accelerated stress testing of multi-source LED products: Horticulture lamps and tunable-white modules.* Report prepared for the U.S. Department of Energy. Available at https://www.energy.gov/sites/prod/files/2018/05/f51/ssl_ast-multi-source-led_2018.pdf

earlier study[2] that the stability of royal blue and red LEDs is generally good, which is important to overall product performance because the impact of instability of an LED chip would be significant. Specifically, minimal peak shifts occurred in direct-light emissions from LEDs, and radiant flux remained high (greater than 90% for the MULTI-WT1 DUTs and MULTI-H2 DUTs). The phosphors in this study were less reliable, with the warm white phosphors (used in the MULTI-WT1 DUTs) prone to chromaticity shifts in the green direction, whereas the red phosphors (used in the MULTI-H1 DUTs) were subject to quenching. Chromaticity shifts were also highly impacted by the LED package, with higher levels of blue irradiation in the cooler MP-LEDs promoting photo-oxidation of polymer resins, which in turn reduced the amount of light reflected from the side walls and out of the package when compared with MP-LEDs with higher phosphor content (e.g., warm white LEDs).

The secondary optics of the products in this study were also found to have significant impacts on chromaticity and radiant flux maintenance. The lenses of the MULTI-H1 and MULTI-H2 DUTs discolored during AST to such a degree that they caused parametric failures for both radiant flux maintenance and chromaticity maintenance due to excessive absorption of primarily blue light. Lens discoloration was promoted by temperature, humidity, blue light irradiation, and spatial variability of irradiation that caused selective lens yellowing in areas of high blue light flux. The secondary reflectors and solder masks also discolored due to temperature, humidity, and blue light irradiation, but the relative impacts of these components were minimal on the chromaticity and radiant flux maintenance of the DUTs.

The electronics of the devices in this study did not exert large impacts on the chromaticity and radiant flux maintenance, but they did impact the overall reliability of the horticulture lamps. Abrupt failure caused by the electrical driver was the cause of failure for five out of the six MULTI-H1 DUTs, but electrical failure only accounted for one failure for the MULTI-H2 DUTs. Although these two horticulture lamp products consumed similar power, the components and/or system design of the MULTI-H2 devices proved to be more reliable than the MULTI-H1 devices. As such, careful attention should be paid to driver electronics.

At the conclusion of these tests, some MP-LED packages were still operating near full capabilities (the LED modules had lumen maintenance greater than 90% and chromaticity shift less than five steps on the standard deviation color matching [SDCM] scale) after 20,000 hrs in 95°C elevated ambient temperatures. This finding suggests generally robust performance of LED packages under proper conditions. However, inclusion of secondary optics and humidity testing (6590) for the horticulture lamps studied in this report forced large chromaticity shifts and low radiant flux maintenances (caused by selective photo-induced lens yellowing, photo-oxidation effects, and phosphor degradation). These findings are helpful for providing guidance for future research efforts aimed at reducing chromaticity shift and radiant flux changes for multi-source LED products.

[2] Davis, J. L., Rountree, K., & Mills, K. C. (2018). Luminous flux and chromaticity maintenance for select high-power color light-emitting diodes. Report prepared for the U.S. Department of Energy. Available at https://www.energy.gov/sites/prod/files/2019/01/f58/ssl_rti_lm80-color-leds_july2018.pdf

Table of Contents

List of Figures

List of Tables

1 Introduction

Multi-source light-emitting diode (LED) products contain two of more sources (i.e., LED primaries) that emit light at different wavelengths. The relative light emissions produced by each LED primary in a multi-source LED product can be fixed to a pre-determined value or adjusted between multiple values depending on the design of the lighting device. A fixed ratio of LED primary emissions is desirable in some products to achieve a continuous spectrum optimized for a specific application (e.g., task lighting, horticultural lighting). The ability to vary or tune the relative light emissions from the LED primaries is desirable for application flexibility such as providing indoor lighting for educational spaces [1] or circadian lighting in healthcare facilities [2]. As shown in **Figure 1-1**, the tuning range of lighting devices with multi-source LEDs is defined by the chromaticity points of the LED primaries—two LED primaries (e.g., warm white and cool white) provide for linear tuning between the chromaticity values of the LED primaries, whereas three LED primaries (e.g., blue, green, and red) provide for non-linear tuning to any chromaticity value within the triangle set by the chromaticity values of the LED primaries [3].

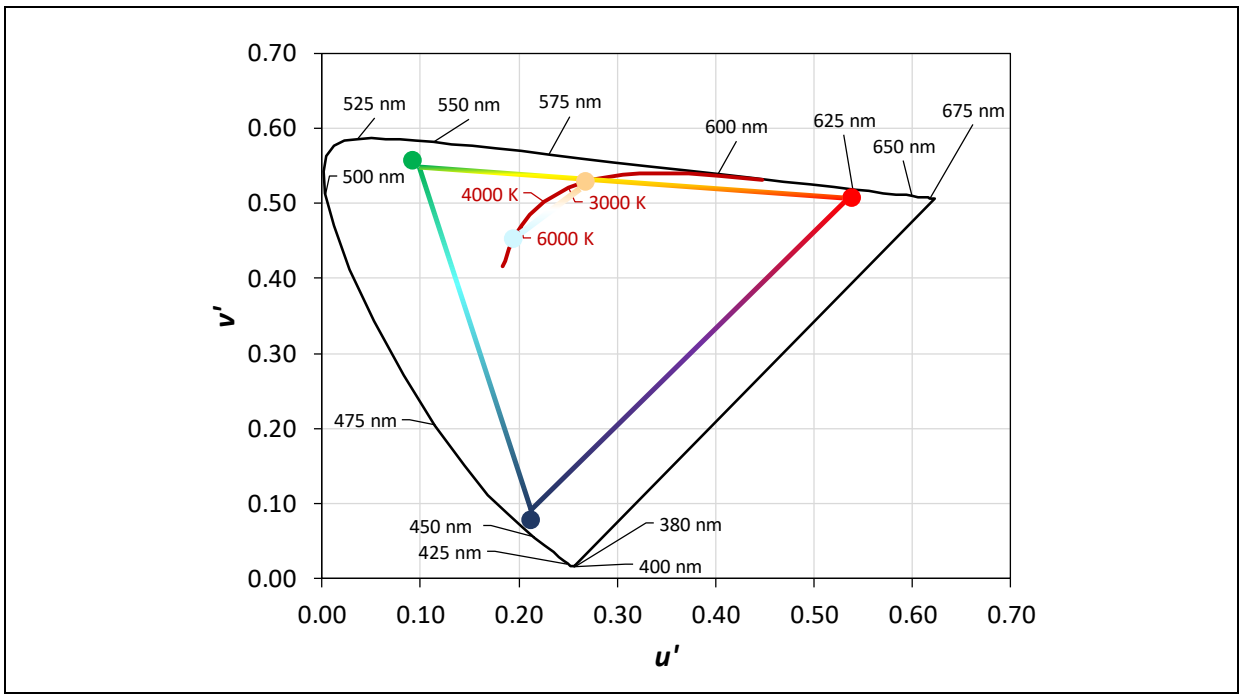

Figure 1-1. A 1976 International Commission on Illumination (*Commission Internationale de l'Eclairage* [CIE]) *u'v'* chromaticity diagram demonstrating the tuning range of multi-source LED products with two LED primaries (i.e., warm white and cool white) and three LED primaries (i.e., blue, green, and red).

Tunable lighting devices for indoor environments provide a variety of potentially beneficial human effects, including promoting circadian alignment, increasing concentration, and improving relaxation [4]. One form of tunable lighting products for indoor applications contains an LED module[3] made from LED packages that produce white light at different correlated color temperature (CCT) values. Such white-tunable lighting (WTL) products can adjust their color between warm white (e.g., CCT is approximately 2,700 K) and cool white (e.g.,

[3] According to the Illuminating Engineering Society's (IES's) definition, an LED module is an assembly of LED packages (components), or dies on a printed circuit board or substrate, possibly with optical elements and additional thermal, mechanical, and electrical interfaces that are intended to connect to the load side of an LED driver. The power source and American National Standard Institute standard base are not incorporated into the device. The device cannot be connected directly to the branch circuit.

CCT is approximately 6,500 K). Alternatively, color-tunable lighting (CTL) can be achieved by using three or more direct-emitting LEDs (e.g., blue, green, red) to provide a broader color gamut for the light source, including saturated colors and different colors of white for lighting [5].

In an analogous manner, multi-source lighting devices provide benefits in horticultural lighting applications and have been shown to promote flowering and leaf growth depending on the lighting spectrum [6]. Horticulture lighting products can be made by using a combination of direct-emitting LEDs to provide emission of blue, red, and deep red wavelengths or phosphor-converted LEDs (pcLEDs) that rely on different phosphor mixtures to provide red and deep-red light emissions. In addition to providing a fixed spectrum that is rich in red and blue, these products can also be designed to provide a tunable lighting spectrum.

The use of multiple LED sources creates new value propositions for LED lighting products that are difficult to achieve with conventional lighting technologies; however, this flexibility also increases the complexity of the lighting system, which can negatively impact reliability. For example, because multi-source LED devices can be operated at different current levels, the luminous flux and chromaticity maintenances of tunable sources will change depending on how much each LED primary is used. In addition, aging of the LED primaries is impacted by the materials used to construct the device and the operating environments (e.g., temperature, humidity, dust particle levels). Clearly, the parameter space required to describe the reliability of multi-source LED devices is large and difficult to model. The best way to understand the impacts of these parameters on the long-term performance of multi-source LED devices is to first examine their probability for occurring (i.e., likelihood), and then determine their relative impacts.

This report focuses on determining the underlying mechanisms responsible for optical changes in multi-source LED products during use. These changes can occur anywhere in the lighting device system, including the LEDs, secondary optics, and electronics. To collect sufficient data to research these failure mechanisms, accelerated stress testing (AST) was used to investigate the degradation that occurs during simultaneous exposure to heat, humidity, and light of different wavelengths [7]. The key parameters examined in this report are luminous flux and chromaticity maintenance of multi-source devices consisting of multiple LEDs.

This document is a follow-up report about multi-source LED products and provides extended data for both WTL and fixed-CCT products [8]. The report focuses on a WTL lighting product (referred to as MULTI-WT1 throughout) and two horticulture growth lamps (referred to as MULTI-H1 and MULTI-H2 throughout). AST data of up to 20,000 hrs are provided for the MULTI-WT1 LED module and up to 8,000 hrs for horticulture lamps (i.e., the fixed-CCT products). Although these data provide detailed information about these lighting devices, the data also provide information about the behavior of the materials used in these devices, which greatly extends the impacts of this research. This report is organized by sections and includes appendices, which are all briefly outlined as follows. **Section 2** provides a summary of the devices under test (DUTs) and the experimental methods used during this study. **Section 3** provides updated findings from AST of MULTI-WT1 LED modules, and **Section 4** provides updated findings regarding horticultural DUTs. **Section 5** discusses the optical failure modes, their probability to occur, and their impacts. **Section 5** also provides insights into how the findings from this study apply broadly across LED devices. **Section 6** presents overall conclusions from this analysis. **Appendix 1** of this report discusses the chromaticity shifts observed for all experiment conditions of the MULTI-WT1 modules.

2 Experimental Methods

The experimental methods and test devices in this report are the same as those described in detail in our previous report (Round 1), although the test duration has been significantly lengthened [8]. These devices are shown in **Figure 2-1**.

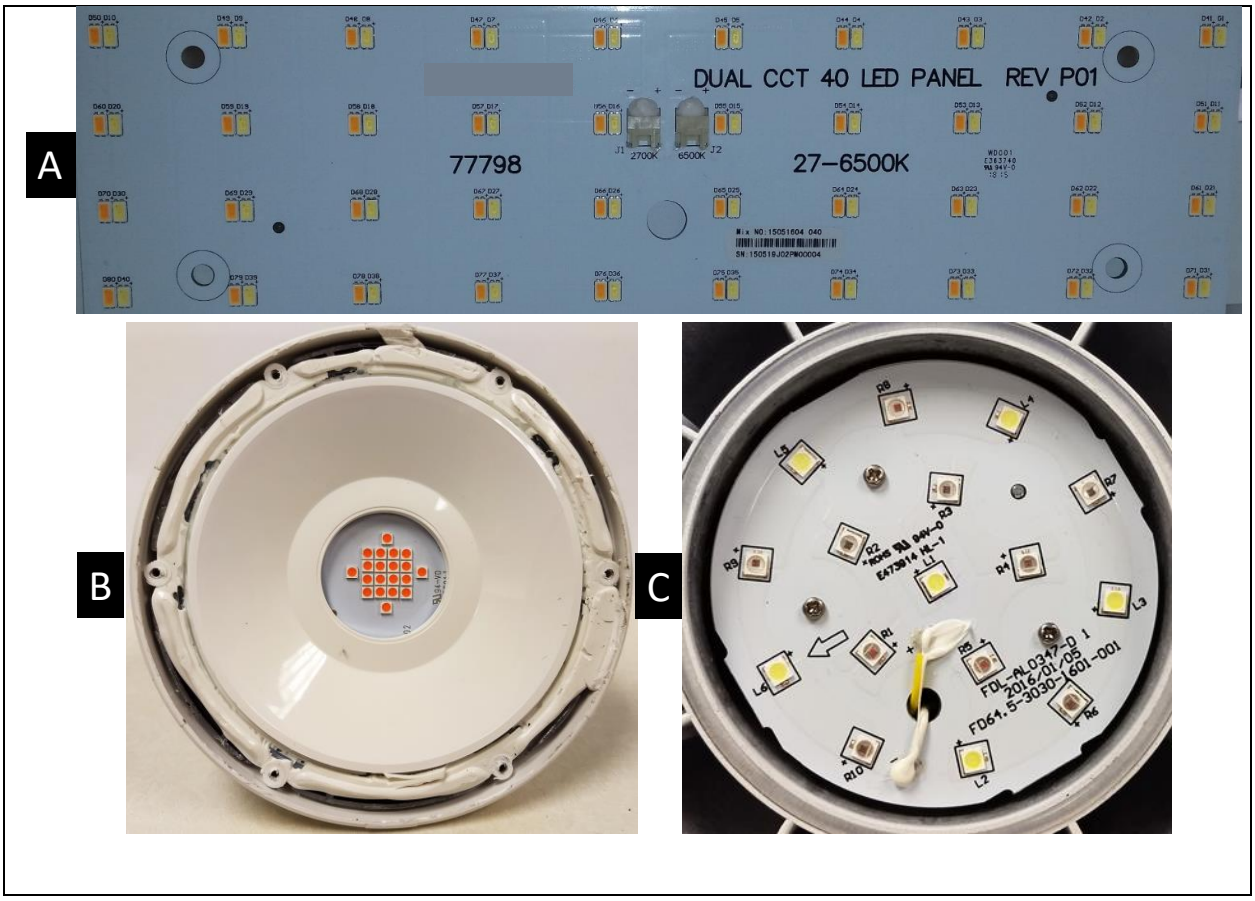

Figure 2-1. The devices examined during this study and discussed in this report include (A) MULTI-WT1 LED modules, (B) MULTI-H1 PAR38 lamps, and (C) MULTI-H2 PAR38 grow lamps.

The MULTI-WT1 LED modules contained 40 warm white LED packages (nominal CCT value of 2,700 K) and 40 cool white LED packages (nominal CCT value of 6,500 K) arranged in couplets on the printed circuit board (PCB) of the module as shown in **Figure 2-1A**. The LEDs used in this module are mid-power LEDs (MP-LEDs), and the molding resin employed in the package is believed to be polycyclohexylenedimethylene terephthalate (PCT), which is a higher performing molding resin than polyphthalamide (PPA) [9]. Standard reflow soldering methods are used to attach the LED packages to the PCB. During AST, separate populations of WTL LED modules were subjected to elevated ambient environments of either 75°C or 95°C. The populations at each temperature were further subdivided by forward current with two LED modules operated at 350 mA, two LED modules operated at 700 mA, two LED modules operated at 1,000 mA, and two LED modules operated at 1,500 mA. Each sample was power cycled for 1 hr on-time and 1 hr off-time. In addition, an identical LED module, which was not exposed to the elevated ambient environment, was kept separate as a control.

Two different types of horticulture lamps were tested, and each contained MP-LEDs arrayed on metal-core PCBs. The MP-LED packages used in these products are believed to have been made from PPA resin. The MULTI-H1 PAR38 lamp shown in **Figure 2-1B**, consisted of only pcLED packages that provided both blue and red emissions in a pcLED package architecture. The MULTI-H2 PAR38 grow lamp shown in **Figure 2-1C**, consisted of a mixture of red direct-emitting MP-LED packages and white-emitting pcLED MP-LED packages that provide blue and green emissions. During AST, six samples of each horticulture lamp product were inserted into a temperature and humidity chamber operating at 65°C and 90% relative humidity (6590). These test conditions were chosen because high humidity and elevated ambient temperatures are often

encountered in horticulture facilities. During operation, the horticulture lamp DUTs cycled on for 2 hrs and off for 2 hrs, and no dimming was applied to the devices.

Photometric testing of the samples and their controls was performed in a 65-inch integrating sphere calibrated with National Institute of Standards and Technology (NIST)–traceable flux standards. All samples were corrected for self-absorption using a control (i.e., unused) sample and an auxiliary lamp. The method does not compensate for changes in increases of self-absorption of the DUTs, such as yellowing, that occur during aging because the control has minimal self-absorption. However, because the interior surface area of the integrating sphere is much larger than that of samples examined in this study, the impacts of surface discoloration of the DUTs is expected to be small and within experimental error. For example, the surface area of the MULTI-WT1 LED modules used in this study were calculated to be approximately 0.5% of the total surface area of the sphere. Consequently, compensating for self-absorption by using an unexposed control samples provides a sufficient method to measure luminous flux changes from the LED packages in the modules.

The photometric properties of each DUT were measured periodically after each AST experiment. All photometric testing was performed with the DUT initially equilibrated to room temperature. Each DUT was then operated for at least 30 minutes prior to measurement to allow for thermal equilibration. During photometric measurements, all of the MULTI-WT1 LED modules were operated at 700 mA regardless of the currents used during elevated temperature exposure. The horticulture lamp DUTs were operated from line mains (120 V alternating current) during all tests. Power consumed, current, voltage, and power factor were measured for each DUT during photometric testing.

Diffuse reflectance and diffuse transmittance of MULTI-WT1 and MULTI-H2 samples over the visible wavelength range were acquired by using a Cary 5000 ultraviolet visible absorption (UV-Vis) near infrared (NIR) spectrophotometer (Agilent Technologies) equipped with an Internal-DRA 2500 diffuse reflectance accessory (Agilent Technologies). The spectrophotometer and the diffuse reflectance accessory were calibrated by using NIST-traceable standards Because of this calibration, absolute diffuse reflectance and absolute diffusion transmittance measurements could be collected of reflective surfaces and lenses used in solid-state lighting (SSL) devices. Diffuse transmittance of the outer concentric lenses of the MULTI-H1 samples were also acquired by using the Cary 5000 UV-Vis-NIR spectrophotometer, but the diffuse transmittance of the concave inner lenses for the MULTI-H1 samples could not be acquired in this manner due to geometrical limitations of the diffuse reflectance accessory on the Cary 5000 UV-Vis-NIR spectrophotometer. Instead, this data was acquired using a 10-inch integrating sphere equipped with a spectrometer following the guidelines from CIE 130-1998 [10].

3 Multi-source LED Products: White-Tunable Modules

In the previous Round 1 report, the luminous flux and chromaticity maintenance of two-chip white-tunable LED modules were presented [8]; the details presented in this current report extend the previous findings to 20,000 hrs of AST. **Section 3** of this report is organized in subsections, which are briefly outlined as follows. **Section 3.1** discusses the visible physical changes in the LED modules. **Section 3.2** describes changes in luminous and radiant fluxes. **Section 3.3** discusses spectral changes in the samples. **Section 3.4** discusses the differences in chromaticity shifts.

3.1 Physical Changes in the Samples

The LED modules experienced two visible physical changes during the 20,000 hrs of AST. First, the solder mask on the LED modules changed from a white appearance to a darker color as shown in **Figure 3-1**. Second, even though the warm white and cool white LED packages were side-by-side on the LED module (see Figure 2-1) and experienced the same currents and temperatures during AST, package discoloration and cracking only occurred on the cool white LED packages.

The test conditions exerted a significant impact on the absolute reflectance from the LED modules, and the diffuse reflectance of a typical DUT is presented in **Figure 3-2**. The change in diffuse reflectance of the PCB occurred in the solder mask, and the largest changes occurred at low wavelengths (less than 550 nm), where there was a significance decrease. Above 550 nm, the difference in diffuse reflectance of the control and DUTs was minimal, even after 20,000 hrs of AST. The change in reflectance eventually reached a limiting value, regardless of experimental conditions. However, the rate of change in diffuse reflectance up to these limiting values was found to depend on temperature and forward current. It took approximately 8,000 hrs for the diffuse reflectance of the solder mask to reach its limiting value for mild test conditions (e.g., 75°C and 350 mA), whereas these changes were complete much sooner under higher stress conditions (e.g., 95°C and 1,500 mA).

Figure 3-1. The control MULTI-WT1 LED module (top) and a second module (bottom) after 20,000 hrs of exposure to the 95°C elevated ambient temperature.

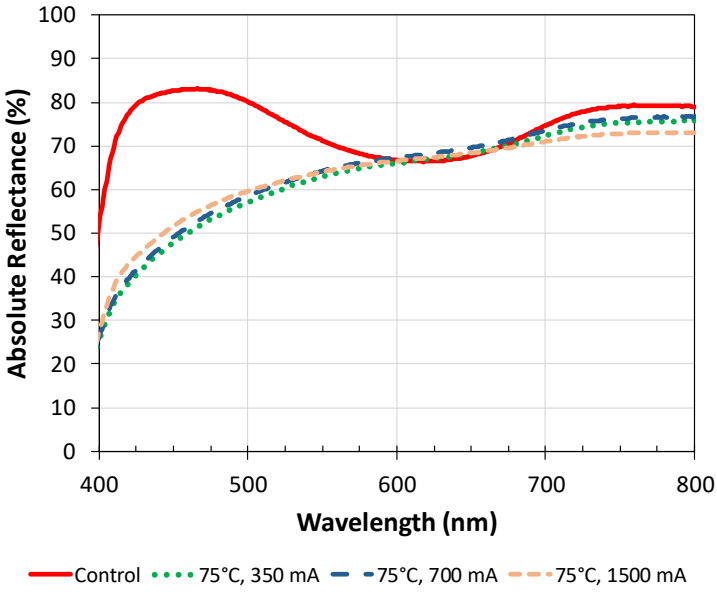

Figure 3-2. Reflectance of the solder mask of the control MULTI-WT1 LED module (solid red line) and similar modules after testing for 20,000 hrs in the 75°C elevated ambient environment at different forward currents. For convenience, the back of the LED module was used for measuring reflectance.

The change in reflectance of the solder mask had a minimal impact on the luminous flux of the LED modules when measured in the integrating sphere, as discussed in **Section 3.2**. The luminous flux was impacted minimally because the LED modules were measured in a 65-inch integrating sphere (13,273 in^2 internal surface area) and the area of the LED module (44 in^2) constituted less than 1% of the total internal surface. This explanation is consistent with our previous finding that the impact of degradation on internal reflective surfaces is dependent upon the luminaire design and the size of the reflective surface in the luminaire [11, 12]. Based on previously reported models regarding the impact of reflector degradation on the efficiency of luminaires, the change in average reflectance (R) in the visible range is expected to reduce the efficiency of a 2 × 2 troffer with a 3-inch optical mixing cavity by a factor of

$$\sqrt{\frac{R}{R_o}}$$

where R_o is the initial average reflectance in the visible range [11, 12]. This model represents an upper limit for the change in luminaire efficiency, and the true value is dependent on the area of the reflector surface (e.g., the solder mask in this case) that is changing and the depth and shape of the optical mixing cavity. Because the average reflectance of the control solder mask was 72% and the average reflectance of the aged solder mask (20,000 hrs of operation in an elevated environment) was approximately 60%, the impact of this material change on luminous flux maintenance+ is expected to be small.

A second physical change that occurred in the MULTI-WT1 DUTs was the appearance of small cracks at the interface of the silicone and molding resin around the edges of the cool white LED packages, as shown in **Figure 3-3**. These cracks were observed after 20,000 hrs at all combinations of temperature and forward current examined in this test, but were only found in the cool white LED packages. Therefore, we concluded that this physical change was caused by the higher blue light content of the cool white LED packages on the DUTS. This finding is consistent with results that show optical and mechanical properties of the molding resins for MP-LED packages and reflector materials will degrade under blue light irradiation [13, 14, 15].

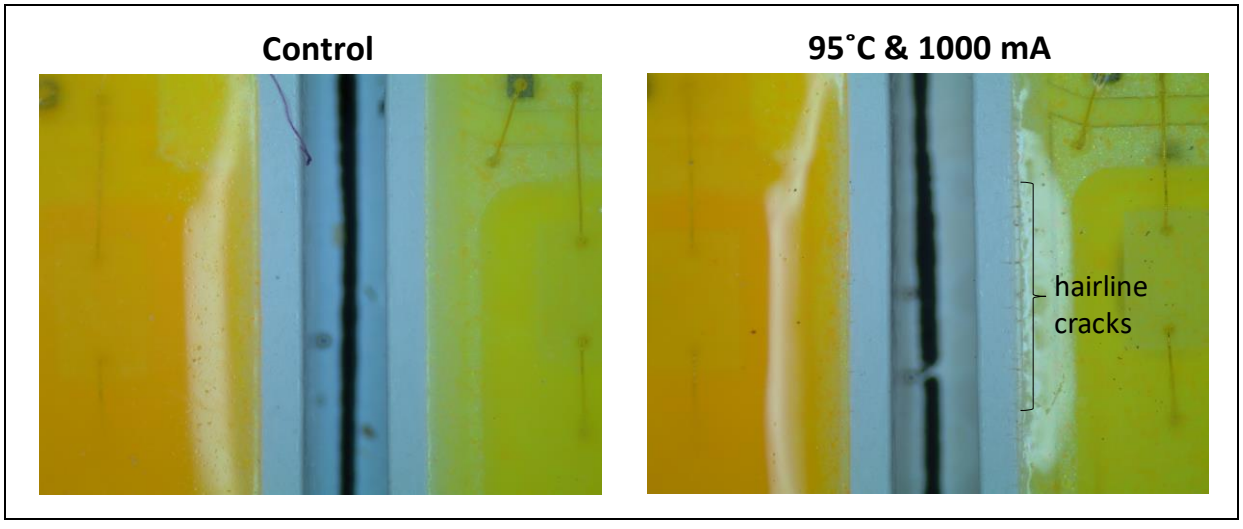

Figure 3-3. Images of the warm white and cool white MP-LEDs from a MULTI-WT1 control module (left) and a second MULTI-WT1 module (right) after 20,000 hrs of exposure at 95°C and 1,000 mA.

3.2 Luminous Flux Changes

The changes in luminous flux maintenance for the warm white and cool white LED primaries, at the different forward currents used in this test, are presented in **Figure 3-4** and **Figure 3-5**, respectively, through 20,000 hrs of testing. Three main trends can be discerned from the luminous flux maintenance data. First, the luminous

flux maintenance of the DUTs remained high (i.e., >0.90), even after 20,000 hrs of testing, except for the 95°C and 1,500 mA DUTs, which were removed from testing after 9,000 hrs. Second, the luminous flux maintenance of the DUTs operated at a forward current of 1,500 mA was consistently lower than that of the DUTs operated at lower currents regardless of the test temperature. Third, there were three distinct regions of luminous flux change as shown in the graphs of Figure 3-4 and Figure 3-5.

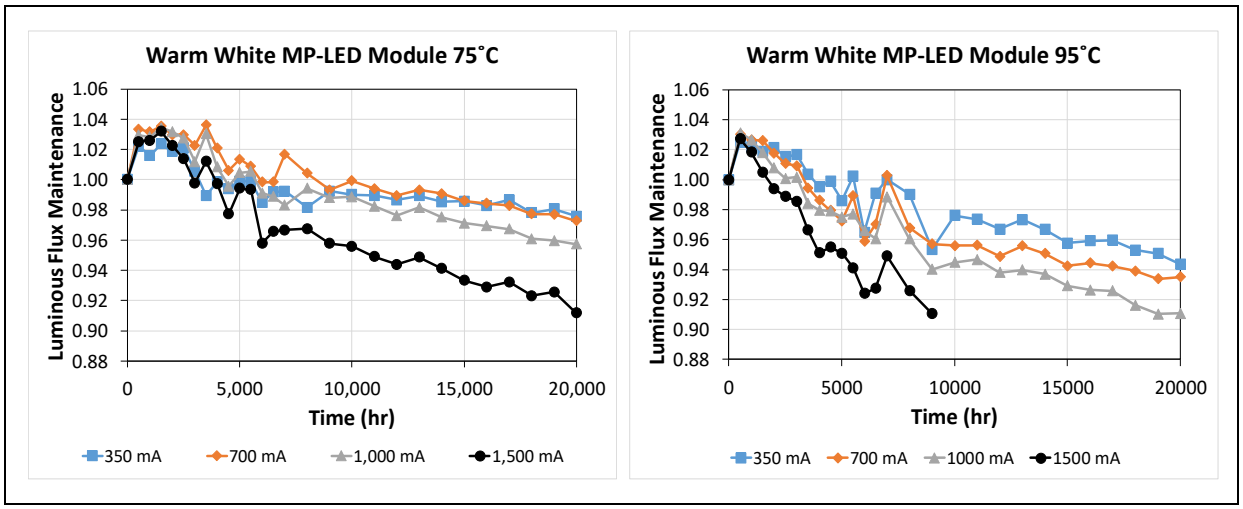

Figure 3-4. Luminous flux maintenance of the warm white LED primaries for MULTI-WT1 in the 75°C (left) and 95°C (right) elevated temperature environments.

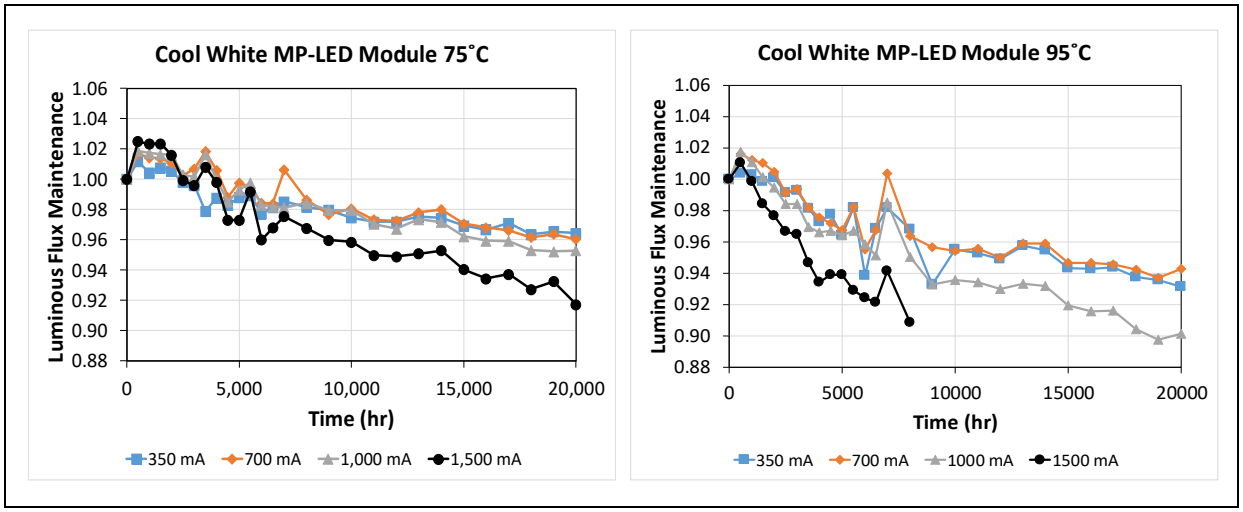

Figure 3-5. Luminous flux maintenance of the cool white LED primaries for MULTI-WT1 in the 75°C (left) and 95°C (right) elevated temperature environments.

The measured luminous flux maintenance of all DUTs tested to 20,000 hrs ranged from 90% to 98%. This level of luminous flux maintenance is excellent, given the relatively harsh test conditions (e.g., ambient temperatures of up to 95°C). For the DUTs tested at 95°C and 1,500 mA, the luminous flux maintenance declined faster than the DUTs tested at less severe conditions, and testing was stopped at 9,000 hrs due to solder interconnect issues. The luminous flux maintenance of these DUTs was approximately 0.91 when testing was halted. The difference in performance between DUTs tested at 95°C and 1,500 mA and those tested at other conditions was significant, suggesting that there is a potential difference in failure mechanisms at 95°C and 1,500 mA. In addition, it is worth noting that the luminous flux of the samples remained high even though discoloration of the solder mask occurred, as discussed in **Section 3.2**. When the luminous flux was

measured in the 65-inch integrating sphere, the impact from yellowing of the solder mask on the LED module produced no more than 1% loss of total luminous flux due to the relative surface areas of the DUT and the sphere interior. Therefore, the yellowing of the solder mask is a minor contributor to the loss of luminous flux in the testing setup used in this report, and the major source of luminous flux loss is believed to be mechanisms within the package.

For the test conditions examined in this study, the luminous flux maintenances of DUTs operated at 300 mA and 700 mA during AST were very similar. The luminous flux maintenance of DUTs operated at 1,000 mA during AST was close to (and in some cases overlapped) values from DUTs operated at lower currents in AST. However, luminous flux maintenance for DUTs operated at 1,500 mA during was distinct from DUTs for the other three currents at elevated ambient temperatures of both 75°C and 95°C. A current of 1,500 mA for the LED module corresponds to 150 mA at each LED package, which is near the limits specified by the LED manufacturer (85°C ambient temperature and 180 mA forward current).

Finally, a closer examination of the luminous flux graph shows that there are three distinct regions of luminous flux maintenance, which is consistent with earlier findings for LEDs [16]. These regions are identified as follows:

- Region 1—The emission efficiency increased during the initial operation of the DUT, and the luminous flux maintenance exceeded 1.0.
- Region 2—The luminous flux maintenance began to decrease from its maximum value at an approximately linear rate.
- Region 3—The decrease in luminous flux maintenance changes to a slower rate than in Region 2.

The initial increase in efficiency that happened during Region 1 occurred rapidly and was completed by 1,500 hrs for the DUTs. A bounded exponential function was the best model to account for this behavior [17]. The DUTs then entered a region of steady luminous flux decline, which also corresponded to the time when yellowing of the solder mask occurred. This region of the luminous flux maintenance behavior is classified as Region 2. By 8,000 hrs, the rate of change in luminous flux maintenance for all DUTs decreased relative to that observed in Region 2, and the devices exhibited Region 3 behavior, which lasted for the remainder of the experimental time. Testing to 20,000 hrs confirmed that the decline in luminous flux remained low throughout the test period for these elevated ambient temperature settings. Long-term luminous flux performance was projected using the TM-21-11 procedure (i.e., only data acquired between 10,000 and 20,000 hrs were used to project long-term performance for these DUTs) [18]. As a result, only data measured during Region 3 are used to calculate the α and B values in this case.

The strengths of the solder joints were measured using a shearing fixture on both warm white and cool white packages at the end of testing. Inconsistent results were obtained during these tests, and the resin on the MP-LED packages generally broke before the solder joints. This finding suggests that the solder joints on these DUTs were as strong as can be measured. However, some intermittent solder joint failures were found after 9,000 hrs of testing on LED modules operated at 95°C and 1,500 mA, as previously described in the Round 1 report, and these DUTs were removed from testing [8]. None of the other DUTs displayed this behavior. Specifically, through 20,000 hrs of testing, this failure mode did not occur in any other DUTs in the 95°C test that were operated at forward currents below 1,500 mA. Likewise, the same phenomenon did not occur in the DUTs operated at 1,500 mA (or any other current) in the 75°C environment through 20,000 hrs of testing. Solder joint failure generally occurs through a wear-out mechanism that involves a combination of mismatch expansion between the solder pads on the LED module and the LED package, which creates strain on the solder joint, and the formation of sufficient quantities of specific copper-tin (Cu-Sn) intermetallics, which increase the brittleness of the solder joint and contribute to failure [19]. Although it is highly probable that all samples produced Cu-Sn intermetallics during operation, the fact that no other solder failures were observed to date suggests that this process proceeded at a significantly slower rate in these samples. There seems to be

something unique about the 95°C and 1,500 mA test conditions that promotes this failure mode, and its absence at other test conditions suggests that it is less likely to occur under normal operating conditions of these LED modules.

3.3 Spectral Changes

During testing, the spectra of the warm white and cool white LED primaries changed in different ways, and the rate of these changes varied with the forward current and the elevated ambient temperature of the DUTs. These findings are suggestive of different chromaticity shift modes (CSMs) occurring in the warm white and cool white LED primaries due to the combined effects of phosphor and packaging materials. A comparison of the changes in spectral power distributions (SPDs) from the initial reading of the LED modules to those taken after 2,500; 5,000; 10,000; 15,000; and 20,000 hrs of exposure are presented for the warm white LED primary (**Figure 3-6**) and the cool white LED primary (**Figure 3-7**) of the DUTs. In these figures, SPDs from separate DUTs at a relatively benign condition (75°C and 700 mA) and a more aggressive test condition (95°C and 1,000 mA) are shown. In all cases, the major change in the spectra was a continual reduction in light emissions between the 500 to 800 nm region, which is where phosphor emissions occur. At the higher temperature, the emission from the phosphor tended to decrease at a faster rate than was observed at lower temperatures, but the same change occurred.

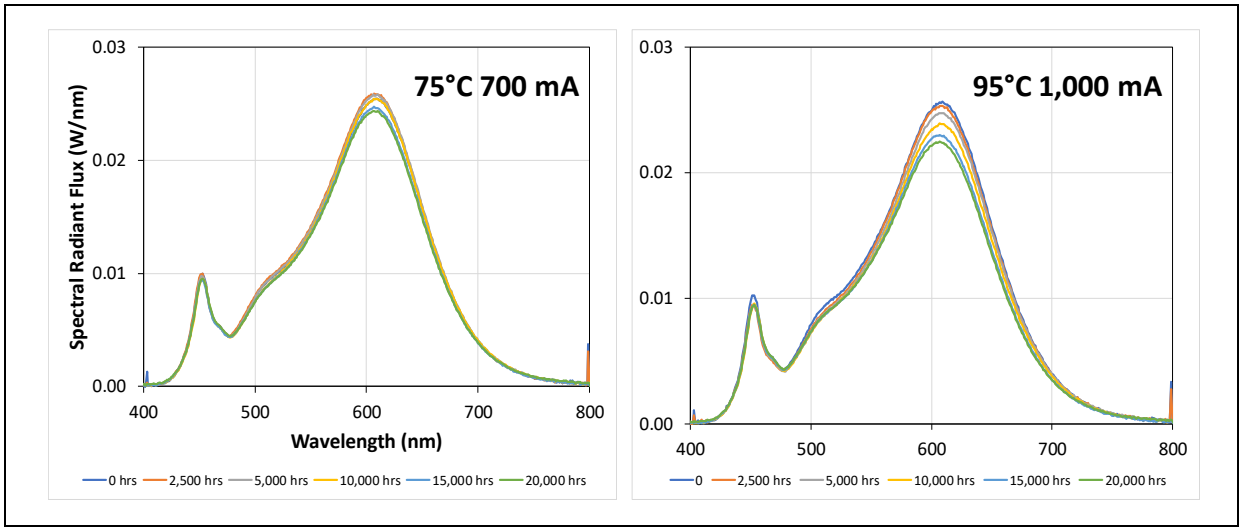

Figure 3-6. Comparisons of the changes in the SPDs of the warm white LED primary for MULTI-WT1 DUTs in 75°C (left) and 95°C (right) elevated ambient temperature testing.

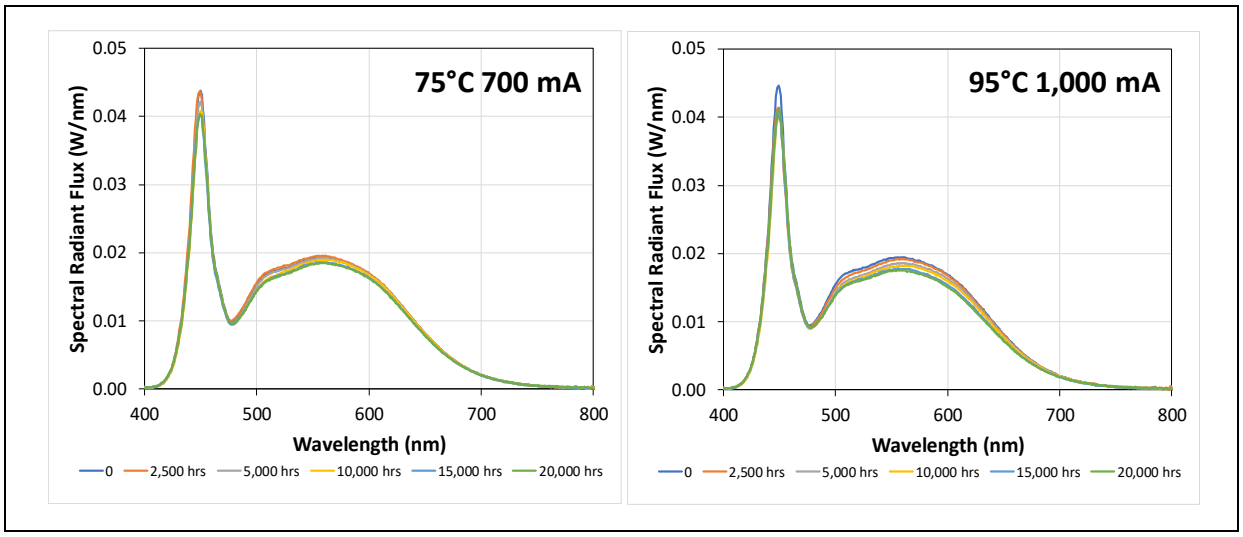

Figure 3-7. Comparisons of the changes in the SPDs of the cool white LED primary for MULTI-WT1 DUTs in 75 °C (left) and 95 °C (right) elevated ambient temperature testing.

For the warm white LED primary on the DUTs, two additional spectral changes occurred beside the reduction in radiant flux emissions from the phosphor used in these devices. First, there was a small change in the radiant flux produced by the blue LED and emitted from the warm white package. Under low stress conditions, the spectral radiant flux of blue light increased during the first 2,500 hrs, and then began a steady decline that continued until 10,000 hrs before it stopped. For the DUTs tested at 95°C and 1,000 mA, a small initial drop in the blue spectral radiant flux occurred and was complete by 2,500 hrs, and the value stabilized after that time. The second additional spectral change was a consistent shift of the phosphor emission peak to shorter wavelengths. As previously discussed, this shift is due to oxidation of the warm white phosphor, resulting in the shift of secondary emissions to shorter wavelengths [20]. This chemical degradation is less significant in many phosphors used in higher CCT LEDs (e.g., cerium-doped yttrium aluminum garnet [YAG:Ce]) because of the higher thermal stability and moisture resistance of these materials.

For the cool white LED primary on the DUTs, the light emissions from both the blue LED and the phosphor decreased, but at different rates. As shown in Figure 3-7, the decrease in spectral radiant flux of blue emissions tended to occur mainly during the early operation of the device, and only minor changes were observed after 5,000 hrs. In contrast, the spectral radiant flux emissions from the phosphor exhibited a consistent decrease over time, but with no change in peak shape. Photo-oxidation of the resin-covered walls of MP-LEDs has been shown to lead to a reduction of phosphor emissions producing a relative enhancement of blue emissions [13]. This finding suggests that blue emissions remain relatively constant after an initial drop, while the change in phosphor emissions is the primary contributor to the loss of luminous flux.

3.4 Chromaticity Shifts

Significant differences were observed in the chromaticity shift behaviors of the warm white and cool white LED primaries of the DUTs, and these differences align with the spectral differences discussed in **Section 3.3**. Representative examples of the different behaviors are shown in **Figure 3-8** for the warm white and cool white primaries on DUTs operated at 1,000 mA and 95°C. The chromaticity shift data for all experimental conditions examined in this study are provided in **Appendix 1**.

Although the chromaticity shift direction of an LED package may change during early life, a single, dominant chromaticity shift usually exists and controls the final direction of chromaticity change and ultimately determines how long it takes for a chromaticity shift of a pre-determined magnitude or failure criteria (e.g., total chromaticity shift ($\Delta u'v'$ >0.007) to occur. As previously discussed, the dominant chromaticity shift

does not immediately occur but may take several thousands of hrs of use to appear [8, 21]. The time at which the dominant chromaticity shift appears is termed the "emergence time," and the value of the emergence time provides a measure of how fast the chromaticity shift is progressing. A closer examination of the data in Figure 3-8 and **Appendix 1** shows that the dominant chromaticity shift for the warm white LED primary was in the green direction, whereas that of the cool white LED primary was in the blue direction. Both types of LEDs exhibit different chromaticity shifts early in testing, but the green shift (for warm white LEDs) and the blue shift (for cool white LEDs) were persistent and still occurring after 20,000 hrs of testing.

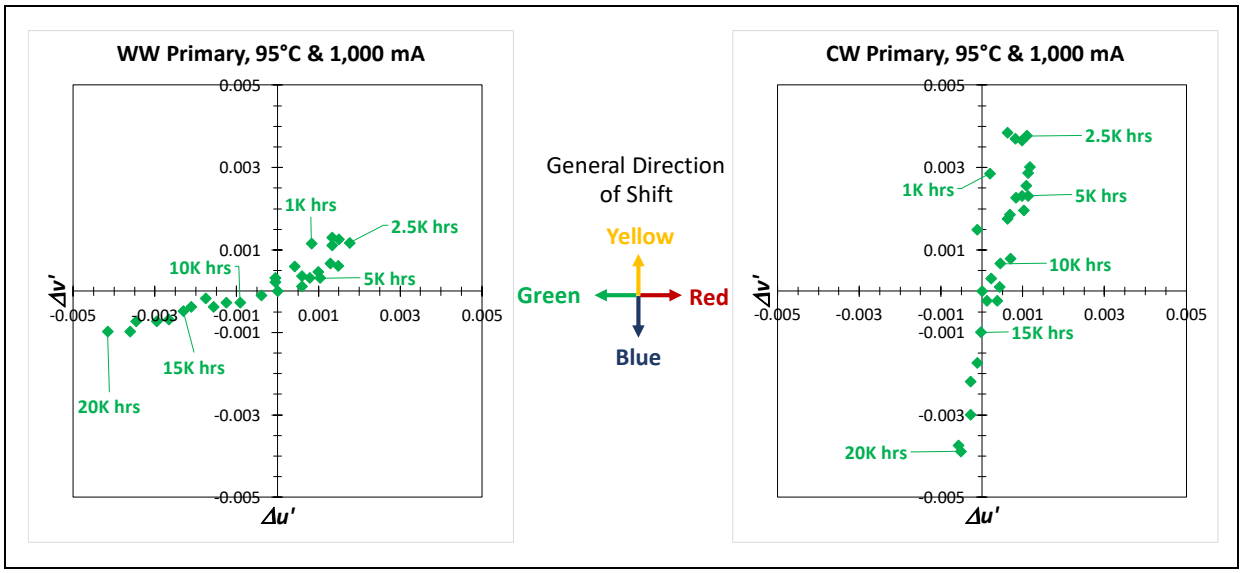

Figure 3-8. Chromaticity shifts for warm white primaries (left) and cool white primaries (right) from a MULTI-WT1 DUT operated at 1,000 mA in the 95 °C temperature condition.

For the warm white primary on the DUTs operated at 1,000 mA in the 95°C elevated ambient temperature environment, the initial chromaticity shift was generally in the yellow direction, and a maximum value was reached ($\Delta u' = 0.0018$ and $\Delta v' = 0.0012$) after approximately 2,500 hrs (see **Appendix 1**). After this time, the shift began to reverse direction, and the shift mainly involved a change in the $-\Delta u'$ direction with minimal change in along the v' axis. This behavior indicates that the dominant chromaticity shift for the warm white primary of the DUTs can be classified as a CSM-2 (i.e., green shift) [22]. This shift has been attributed to changes in the emission properties of the warm white phosphor [12, 22]. After 20,000 hrs of testing at 95°C and 1,000 mA, the total chromaticity shift of the warm white primary in $\Delta u'$ was −0.0042, and the shift in $\Delta v'$ was only −0.0010. The decrease in the $\Delta u'$ chromaticity coordinate exhibits approximately logistic behavior starting at 2,500 hrs for the 95°C and 1,000 mA conditions, which is in agreement with analytical models for chromaticity shift [8, 21]. Other test conditions exhibited the same trend, although the emergence time for CSM-2 shift progressed to longer times as temperature and forward current were reduced. A compilation of the emergence times for the CSM-2 shifts of the warm white LED primary for the DUTs examined in this study are listed in **Table 3-1**.

Table 3-1. Emergence times for the CSM-2 shift of the warm white LED primary for the MULTI-WT1 DUTs.

Test Conditions	Emergence Time for CSM-2 Shift
75°C and 350 mA	>20,000 hrs
75°C and 700 mA	9,000 hrs
75°C and 1,000 mA	6,000 hrs
75°C and 1,500 mA	4,500 hrs
95°C and 350 mA	5,000 hrs
95°C and 700 mA	3,500 hrs
95°C and 1,000 mA	2,500 hrs
95°C and 1,500 mA	1,500 hrs

For the cool white primary on the DUTs, the initial chromaticity shift was generally in the blue direction, which can be observed during the mildest test condition (i.e., 350 mA and 75°C) but was not observed at the measurement times for other experimental conditions. The chromaticity shift then proceeded generally in the yellow direction, but eventually changed permanently to the blue direction. For example, up to 2,500 hrs at 1,000 mA and 95°C, the shift was toward the generally yellow direction, and a maximum value was reached ($\Delta u' = 0.0011$ and $\Delta v' = 0.0038$) for these test conditions. After this time, the shift began to reverse direction and involved mainly a change in the $-\Delta v'$ direction with minimal change in u'. This behavior indicates that the dominant chromaticity shift can be classified as a CSM-4 (i.e., blue shift) because there was an initial, short blue shift, followed by a yellow shift, and culminating with a final blue shift [22]. This shift was attributed to changes in the MP-LED packaging materials due to heat and blue light irradiation [13, 22]. After 20,000 hrs of testing at 95°C and 1,000 mA, the total chromaticity shift of the cool white primary in $\Delta u'$ was only −0.0006, but the shift in $\Delta v'$ was −0.0037. Other test conditions exhibited the same trend, although the emergence time for CSM-4 shift became longer as temperature and forward current were reduced. A compilation of the emergence times for the CSM-4 shifts of the cool white LED primary of the DUTs examined in this study are listed in **Table 3-2**.

Table 3-2. Emergence times for the second blue shift for CSM-4 behavior in the cool white LED primary for the MULTI-WT1 DUTs.

Test Conditions	Emergence Time for CSM-4 Shift
75°C and 350 mA	15,000 hrs
75°C and 700 mA	15,000 hrs
75°C and 1,000 mA	14,000 hrs
75°C and 1,500 mA	5,500 hrs
95°C and 350 mA	2,500 hrs
95°C and 700 mA	2,500 hrs
95°C and 1,000 mA	2,500 hrs
95°C and 1,500 mA	1,500 hrs

4 Multi-source LED Products: Horticulture Lamps

In our previous Round 1 report [8], we discussed the luminous flux and chromaticity maintenance of several parabolic aluminized reflector (PAR) horticulture lamps, and the details reported here extend the previous findings to encompass radiant flux (in lieu of luminous flux) and chromaticity maintenance until device failure (MULTI-H1) or 8,000 hrs of AST (MULTI-H2). **Section 4** of this report is organized in subsections, which are briefly outlined as follows. **Section 4.1** briefly summarizes the horticulture test methods and lamp properties.

Section 4.2 discusses changes in radiant flux. **Section 4.3** details spectral changes in the samples. **Section 4.4** discusses chromaticity shift differences. **Section 4.5** discusses lens changes for these horticulture lamps. **Section 4.6** presents an overview of other lamp component changes and failure modes.

4.1 Horticulture Lamp Test Methods

An overview of the MULTI-H1 and MULTI-H2 horticulture lamp products investigated in the current study was provided in the previous Round 1 report [8]. These products were investigated because they were commercially available and generated the horticulture spectrum in different ways. The LED modules in the MULTI-H1 DUTs contained pcLEDs with blue LEDs and red phosphors, whereas the MULTI-H2 DUTs contained LED modules comprised of pcLEDs (with direct-emitting blue LEDs and broad-emitting green-yellow phosphors) and direct-emitting red LEDs. The pre-operation electrical properties, chromaticity coordinates, and a description of the LED packages outlined in the earlier report are summarized for convenience in **Table 4-1** of this current report. Although many of the properties of the MULTI-H1 and MULTI-H2 horticulture DUTs are similar (i.e., the LEDs are powered in series, similar radiant power, polycarbonate [PC] lenses, and similar electrical efficiency), there are some unique differences that were noted in our previous report. For instance, the pcLEDs in the MULTI-H1 lamp are comprised of blue LEDs and red phosphor material, whereas the pcLEDs in the MULTI-H2 lamp are comprised of blue LEDs and a green-yellow phosphor material, in addition to red LEDs. Furthermore, although both pcLED packages have two blue LEDs in parallel, the current across the blue LEDs in the MULTI-H1 lamp is approximately 70% that of the MULTI-H2 DUTs. It is also important to note that the red LEDs of the MULTI-H2 DUTs run at a current twice that of the blue LEDs in the MULTI-H2 lamp (because they are in series). Finally, although similar power and efficiency are delivered by the drivers of these two DUTs, the overall size and operating capacity of the PCB and its electrical components of the MULTI-H1 driver are approximately twice as small as the MULTI-H2 driver as shown in **Figure 4-1**.

Table 4-1. Horticulture lamp properties prior to AST.

Properties	MULTI-H1 PAR38 Grow Lamp	MULTI-H2 PAR38 LED Grow Lamp
Output voltage (V)	60.1	41.6
Output current (mA)	230	323
Electrical efficiency (%)	86.8	87.5
Chromaticity coordinates	u' = 0.3819 ± 0.0008 v' = 0.3842 ± 0.0021	u' = 0.2594 ± 0.0031 v' = 0.4548 ± 0.0004
Lens material	PC	PC
LED package configuration	In series	In series
Number of LED packages and type	20 pcLEDs (all MP-LEDs with a blue LED and red phosphor)	16 MP-LEDs (6 pcLEDs and 10 red LEDs)
Radiant power (W)	4.17 ± 0.05	4.60 ± 0.03

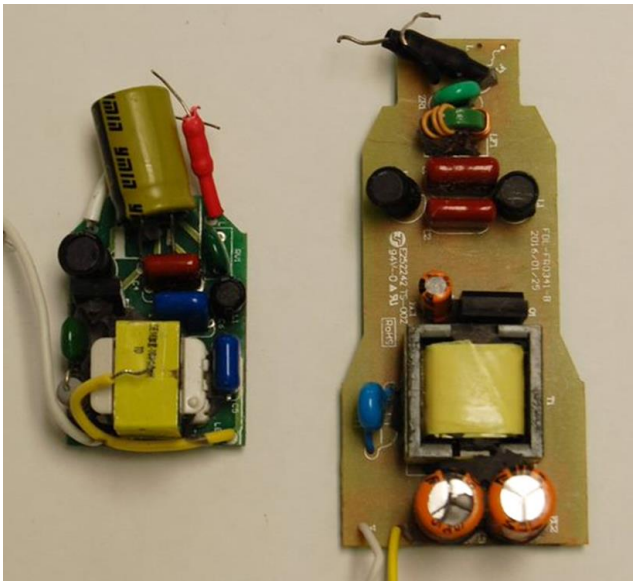

Figure 4-1. The electrical drivers used to power the MULTI-H1 (left) and MULTI-H2 (right) PAR38 horticulture DUTs.

4.2 Radiant Flux Changes

The radiant flux maintenance for all DUTs decreased with exposure time, and the average temporal radiant flux maintenances for the DUTs are shown in **Figure 4-2**. The average radiant flux and error bars were calculated from the six test DUTs for each product unless otherwise noted in the remainder of this section.

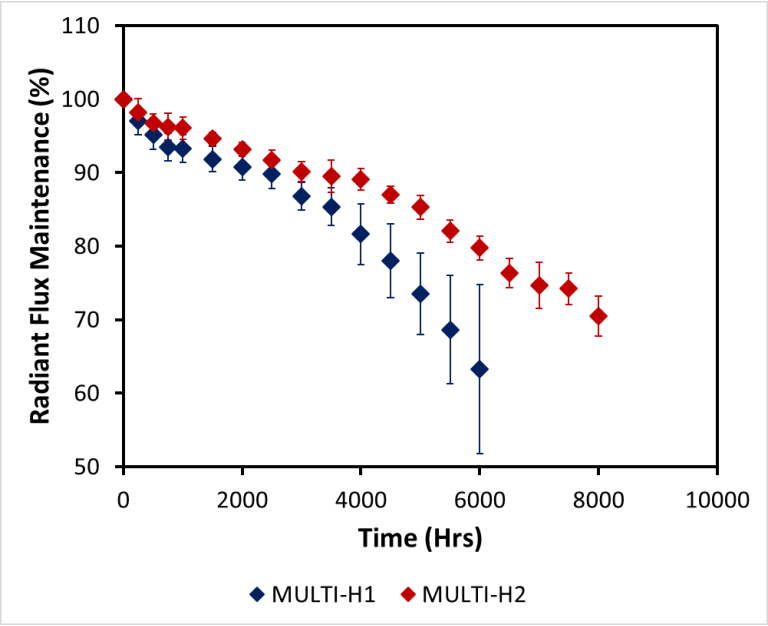

Figure 4-2. Average radiant flux maintenance of MULTI-H1 and MULTI-H2 PAR38 DUTs after aging in 6590.
Notes: Radiant flux maintenance was corrected for variation observed in the control lamp to account for spectrometer and experimental variations. Error bars represent one standard deviation.

The average radiant flux for the MULTI-H1 DUTs was only recorded through 6,000 hrs because these DUTs experienced complete "lights-out" failure by 6,500 hrs of exposure to the 6590 environment. As noted in our previous report [8], the radiant flux of the six MULTI-H1 DUTs decreased quickly at the onset of stress testing. The rapid decrease in radiant flux was followed by a slower period of decrease through 3,500 hrs, and then a sharp, linear decrease in radiant flux was observed from 4,000 to 6,000 hrs. The standard deviation also rapidly increased between 4,000 and 6,000 hrs, which indicates aging in a stress environment. In addition, the larger standard deviations could have resulted from lower population sizes as testing continued: at 5,274 hrs, one of the MULTI-H1 DUTs failed; therefore, the average radiant flux at 5,500 hrs was taken for the five remaining operational DUTs, and then between 5,500 and 6,000 hrs, two more MULTI-H1 DUTs failed so the average radiant flux recorded at 6,000 hrs was the average of the three operational DUTs. Prior to failure at 6,000 hrs, the average radiant flux recorded was 63.3% for the MULTI-H1 devices. The exact times to failure for these devices and the MULTI-H2 DUTs are provided in **Table 4-2**. **Section 4.6** of this report discusses the failure analysis for the DUTs.

All MULTI-H2 DUTs remained in good operating condition through 7,500 hrs, with the first "lights-out" failure occurring at 7,949 hrs. Although many horticulture lamp manufacturers report luminous flux rated lifetime values (e.g., the time at which the light output from the lamp is 70% of the initial luminous flux [L_{70}]), parametric failure will be defined as radiant flux at 70% of its initial value (R_{70}) in this report. This metric is used instead of L_{70} because luminous flux is a measure of the perceived light by humans (and not plants). This distinction is important because four out of the six MULTI-H2 DUTs experienced parametric failure defined by L_{70} by 6,500 hrs, but parametric failure defined by R_{70} was not reached until 8,000 hrs for two out of the six DUTs, and testing was stopped before parametric failure occurred on the other three DUTs (right censored). Due to the lights-out failure prior to 8,000 hrs, the temporal average radiant flux maintenance of 70.5% at 8,000 hrs reported in Figure 4-2 is the average of five MULTI-H2 DUTs.

The depreciation of radiant flux of the MULTI-H2 DUTs followed a similar trend as the MULTI-H1 DUTs (fast initial decay; slower decay through 3,500 hrs; faster decay after 4,000 hrs), albeit the depreciation for the MULTI-H2 DUTs was slower than that of the MULTI-H1 DUTs. The MULTI-H2 DUTs maintained acceptable radiant flux through 7,500 hrs for all six test DUTs, but the average radiant flux for the MULTI-H1 DUTs dropped below R_{70} by 5,500 hrs. In addition, the standard deviation of the radiant flux for the MULTI-H2 DUTs remained small throughout testing, suggesting better uniformity of these samples compared with the MULTI-H1 devices. The lenses of the devices for both products showed continued signs of aging (yellowing and cracking), and it was hypothesized that the difference in these lens shapes may be responsible for the larger reduction and variation in radiant flux observed in the MULTI-H1 DUTs compared with the MULTI-H2 DUTs. **Section 4.5** of this report discusses the effects of the lenses.

Table 4-2. Time to failure or suspension time for the MULTI-H1 and MULTI-H2 DUTs.

DUT Number	DUT Description	Time to Failure or Time to Suspension (Hrs)	Lights out, Parametric, or Right Censored
387	MULTI-H1	5,274	Lights out
413	MULTI-H1	5,867	Lights out
412	MULTI-H1	6,000	Lights out
386	MULTI-H1	6,040	Lights out
410	MULTI-H1	6,041	Lights out
411	MULTI-H1	6,124	Lights out
401	MULTI-H2	7,949	Lights out
377	MULTI-H2	8,000	Parametric
400	MULTI-H2	8,000	Parametric
376	MULTI-H2	8,000	Right censored
402	MULTI-H2	8,000	Right censored
403	MULTI-H2	8,000	Right censored

4.3 Spectral Changes

As mentioned **above**, the average radiant flux maintenance for the MULTI-H1 devices prior to failure at 6,000 hrs was 63.3%. Representative SPDs are shown in **Figure 4-3** of a DUT prior to 6590 exposure and post-6,000 hrs of 6590 exposure (i.e., directly before the device failed). Both direct-emitting blue LED and red phosphor peaks experienced a substantial decrease in spectral radiant flux at the end of aging. To better understand these decreases, the radiant power of each component was calculated and plotted temporally as shown in Figure 4-3. As previously reported, the red phosphor experienced a large drop in radiant power during the initial 500 hrs of testing in 6590. Subsequently, the radiant power attributed to the red phosphor decreased minimally through 3,000 hrs, and then started to decrease at a higher rate from 3,500 hrs to 6,000 hrs. The radiant power attributed to the direct-emitting blue LED declined at a steady rate throughout the AST. From this analysis, it is clear that the shape of the radiant flux maintenance curve previously described (i.e., the rapid, initial decrease in radiant flux, followed by a slower period of decrease through 3,500 hrs, and then a sharp, linear decrease in radiant flux between 4,000 and 6,000 hrs, Figure 4-2) was predominantly influenced by the changes occurring in the red phosphor.

Further analysis of the average spectral peak location of each emitter for the MULTI-H1 DUTs, represented herein as the centroid wavelength, revealed a significant shift in peak location (approximately +2.5 nm) for the blue LED as shown in **Figure 4-4**. The peak position remained stable through 3,000 hrs of aging, and then an exponential increase in peak position occurred. The red phosphor did not experience the same shift in its average centroid wavelength, as shown in Figure 4-4, but rather fluctuated (± 1 nm, with similar behavior as the control sample). The shift in the centroid wavelength of the blue LED suggests that the chromaticity shift of this device may be due to an outside process (i.e., something other than LED or phosphor decomposition).

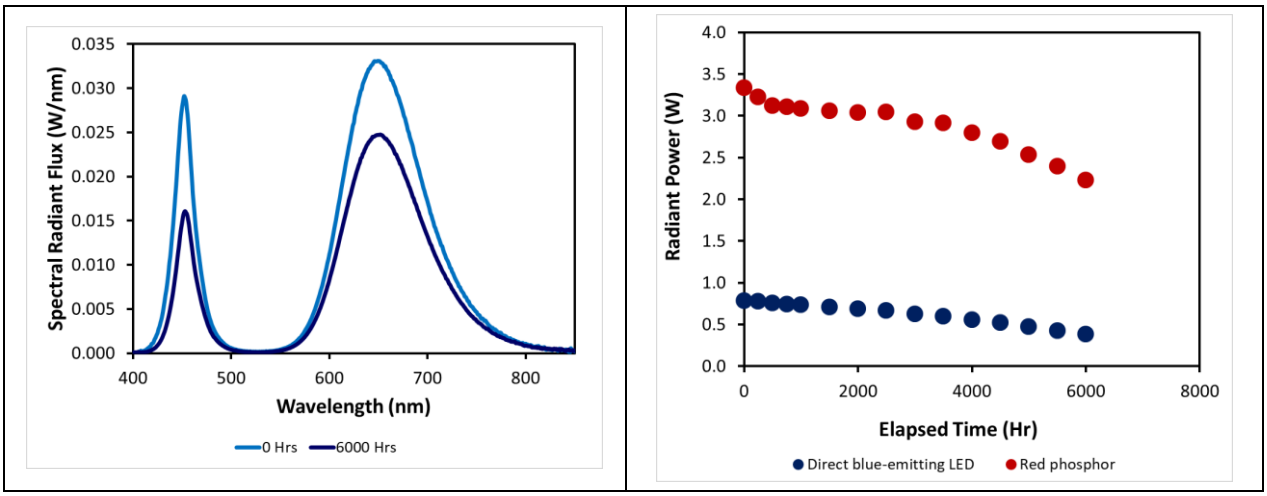

Figure 4-3. Spectral radiant flux of a MULTI-H1 lamp (DUT-386) after aging in 6590 (left) and changes in the radiant power of the direct-emitting blue LED and red phosphor (right).

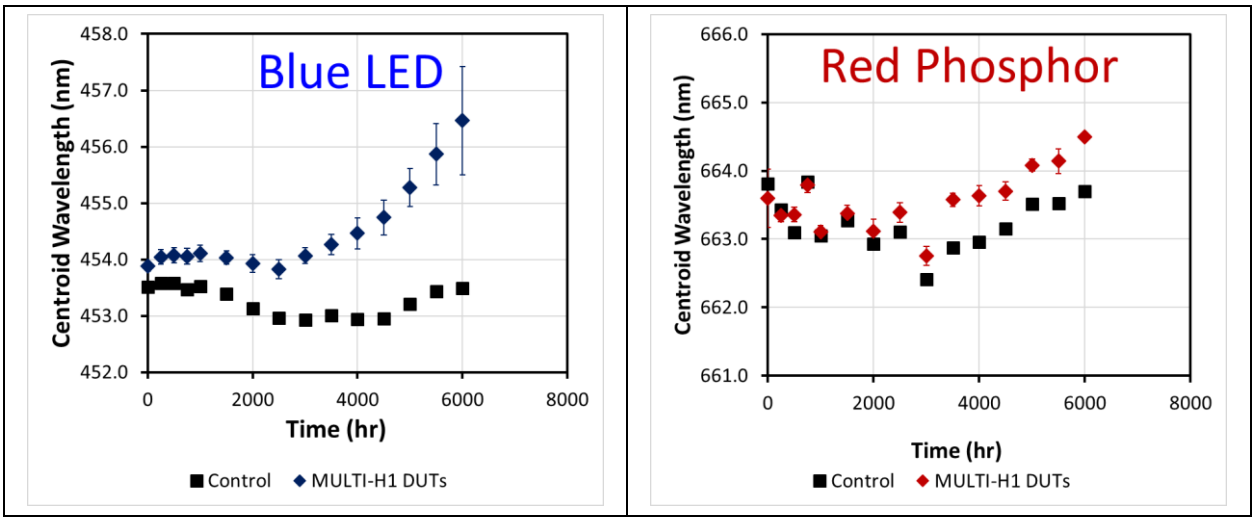

Figure 4-4. Temporal average centroid wavelength of the blue LEDs (left) and red LEDs (right) for the MULTI-H1 DUTs compared with the temporal centroid wavelength of the control device. Findings show a statistically significant increase in blue LED centroid wavelength with aging, but stable red LED centroid wavelength with aging.

As mentioned **above**, the average radiant flux maintenance for the MULTI-H2 DUTs was 70.5% post-8,000 hrs of exposure to the 6590 environment. Representative SPDs are shown in **Figure 4-5** of a DUT prior to 6590 exposure and post-8,000 hrs of 6590 exposure. A calculation of the temporal radiant power from the SPDs indicated that the individual rates of decay for the direct-emitting blue LED and green-yellow phosphor were higher than the rate of decay for the direct-emitting red LED (Figure 4-5). Two regions of decay were observed for the blue LED (slower decay from 0–4,000 hrs and a faster decay from 4,000–8,000 hrs). Three regions of decay were observed for the green-yellow phosphor (fast initial decay to 1,000 hrs, slower decay from 1,000–4,000 hrs, and faster decay from 4,000–8,000 hrs). The radiant power attributed to the red LED was the most stable, and the rate of decay remained constant through AST.

Further analysis of the average spectral peak location for the direct blue emitter revealed a significant increase in peak position (approximately +2.9 nm) by 8,000 hrs of 6590 exposure. Similar to the MULTI-H1 DUTs, the peak position for the MULTI-H2 DUTs remained stable for a period of time before an increase in peak position was observed (the peak position remained stable for 3,000 hrs for the MULTI-H1 DUTs and 4,000 hrs

for the MULTI-H2 DUTs) (**Figure 4-6**). Also, similar to the MULTI-H1 DUTs, the peak position of the direct-emitting red LEDs of the MULTI-H2 DUTs fluctuated with the control sample, albeit the fluctuations were slightly smaller (±0.5 nm) than the MULTI-H1 devices (±1 nm). The peak position of the phosphor green-yellow emitter was not considered here due to its broad nature and the difficulty associated with accurately representing its peak position as radiant flux decreased.

Higher operating temperatures and changes to the current amplitude and/or waveform delivered to the LED modules are known to cause peak shifts in LEDs. Although peak shifts resulting from temperature or current changes between LED primaries of different color (e.g., blue versus red LEDs) do not have the same magnitude, temperature and/or current changes that are large enough to produce a peak shift ranging from 2.5 to 2.9 nm in one LED primary (such as those observed in the blue LED primary for the horticulture lamps studied in this report) are likely to produce a measurable peak shift in the other LED primary because similar temperature and current changes are experienced by the LEDs across the module. Because the red LED primary of the MULTI-H2 DUT did not experience a peak shift, it is unlikely (but still possible) that the shift in centroid wavelength for the blue LED was caused by temperature and/or current changes. Other possible causes of centroid wavelength shift are the formation of a new emitting compound (though this is unlikely in LEDs) and changes in optical components (e.g., reflectors, lenses). The impact of the peak wavelength shift on chromaticity and the cause of the peak shift are discussed later in this section.

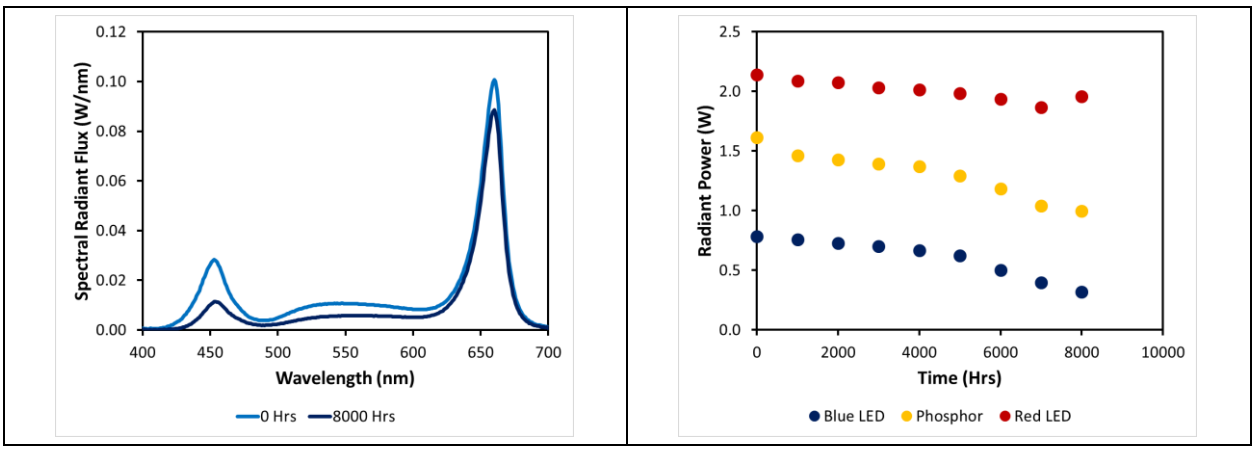

Figure 4-5. Spectral radiant flux of a MULTI-H2 lamp (DUT-376) after aging in 6590 AST (left) and changes in the radiant power of the LED module containing blue and red LEDs and phosphor (right).

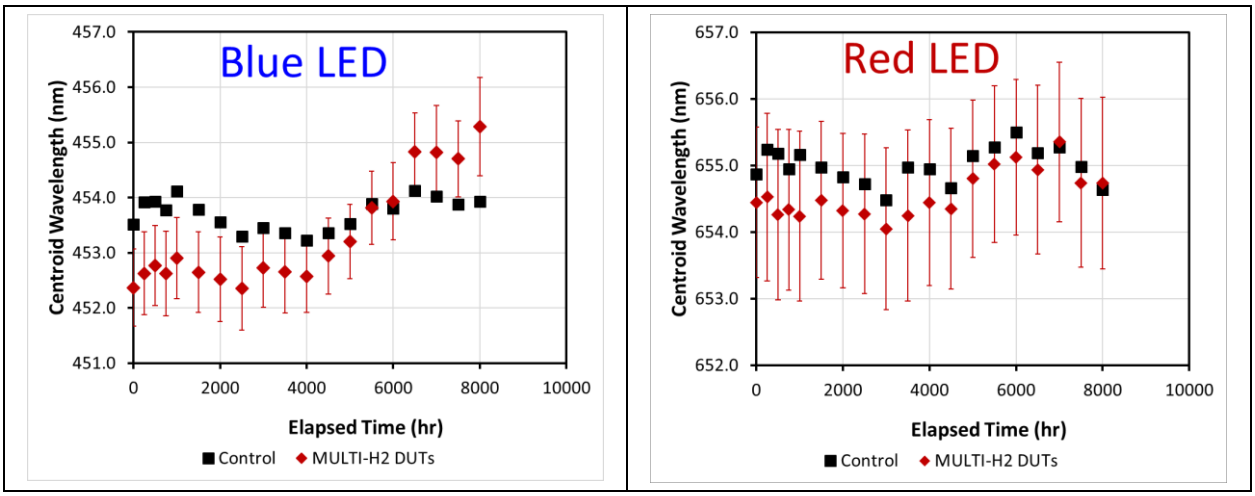

Figure 4-6. Temporal average centroid wavelength of the blue LEDs (left) and red LEDs (right) for the MULTI-H2 DUTs compared with the temporal centroid wavelength of the control device show a statistically significant increase in blue LED centroid wavelength with aging, but stable red LED centroid wavelength with aging.

4.4 Chromaticity Shift and Modeling

The chromaticity shifts experienced by the horticulture lamp DUTs in this current study terminated in the red-yellow direction as shown in **Figure 4-7**. In a previous report, it was noted that the MULTI-H1 DUTs experienced a quick, initial chromaticity shift in the $-\Delta u'$, $-\Delta v'$ (green-blue) direction before a secondary process became dominant at 750 hrs. During the secondary process, the chromaticity shift proceeded in the yellow-red direction until DUT failure, wherein both u' and v' shifted in the positive direction. In contrast, within the first 250 hrs, the MULTI-H2 DUTs experienced a large chromaticity shift in the $+\Delta u'$, $-\Delta v'$ (red-blue) direction. Then the chromaticity shift proceeded along the $+\Delta u'$ axis until approximately 4,000 hrs, after which both chromaticity coordinates shifted in the positive direction (Figure 4-7).

Prior to 4,000 hrs, neither product displayed much variation in chromaticity shift across all six samples, suggesting strong sample uniformity. As the products aged to 6,000 hrs, the chromaticity shift for the DUTs began to vary, with variation increasing more in the u' coordinate relative to the v' coordinate. A smaller magnitude of chromaticity change ($\Delta u'v'$) was observed for the MULTI-H2 DUTs relative to the MULTI-H1 DUTs throughout the lifetime of the MULTI-H1 DUTs (6,000 hrs).

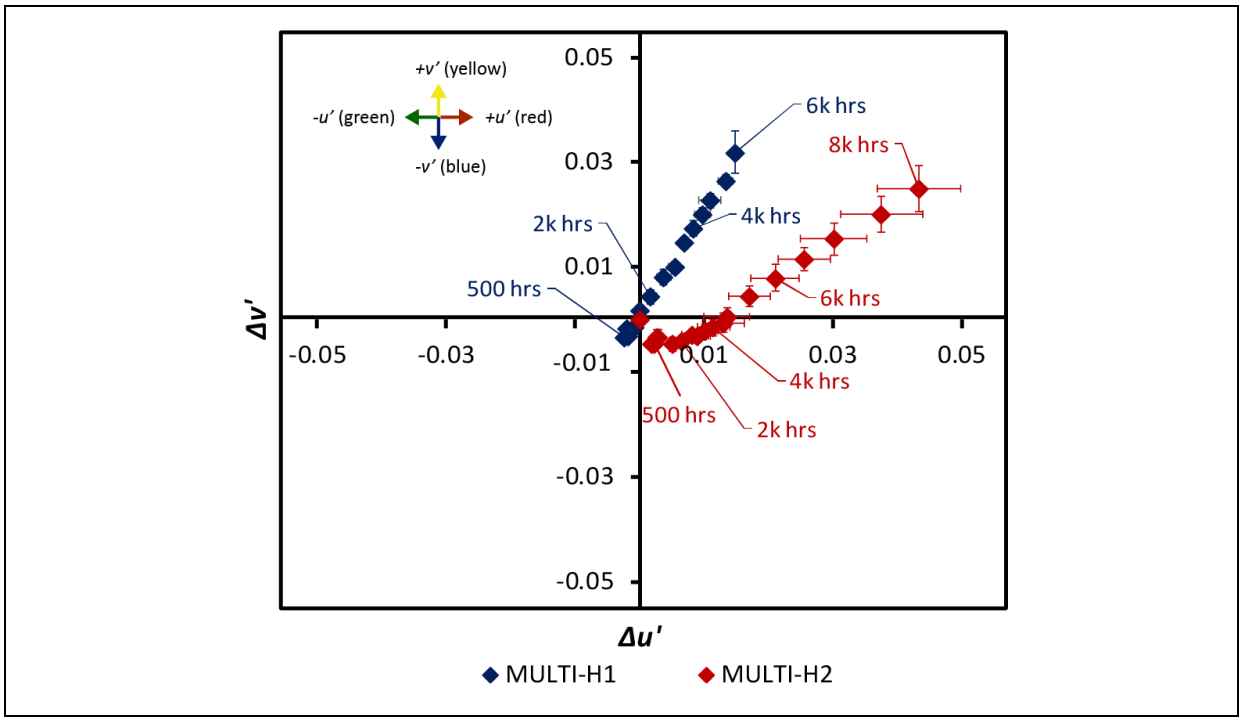

Figure 4-7. Average chromaticity diagram for the DUTs aged in 6590. Note: The variation in average *Δu′* and *Δv′* is represented with one standard deviation.

The temporal behaviors of the *Δu′* and *Δv′* coordinates (through 3,000 hrs) were modeled in a previous report, and the models are updated in this current report. The previous models were optimized by summing one logistic function and one bounded exponential function for each chromaticity coordinate, and it was found that these models continued to represent the data. Optimization was performed with the sum of squared errors (SSE) and least squares methods.

Further inspection of the temporal behavior of the *Δu′* and *Δv′* coordinates supports a two-shift process for the MULTI-H1 DUTs, as shown in **Figure 4-8**. As described in a previous report, there was a rapid initial shift in the *Δu′* component within the first 250 to 500 hrs, wherein the *Δu′* component of chromaticity shift dropped to its lowest value. The negative trajectory of the *Δu′* component of chromaticity shift was short lived, and at approximately 750 hrs, the *Δu′* coordinate began to shift toward positive values. The *Δv′* component also experienced a rapid chromaticity shift in the first 250 to 500 hrs, wherein it too experienced its lowest value. The initial $-\Delta u'$ and $-\Delta v'$ components of chromaticity shift were each fit with a bounded exponential model, and lower asymptotic limits ([*L*], −0.0038 and −0.0040, respectively) were found. Due to the timescale of the reaction, the initial chromaticity shift in the $-u'$ and $-v'$ direction was caused by the initial loss of emission attributed to the red phosphor (Figure 4-3) whereas the shift in the yellow-red direction is due to the loss of blue emissions

After the rapid initial chromaticity shifting process, the dominant chromaticity shift occurred at an emergence time of 500 hrs and continued through the end of MULTI-H1 DUT life. The dominant chromaticity shift was a slower process than the initial chromaticity shift, and *Δu′* and *Δv′* components of chromaticity shift increased until the end of device life (Figure 4-8). The dominant process was best fit with a logistic model and, although device failure occurred before an exact termination point for the second chromaticity shift could be determined, the model suggests a termination point of $\Delta u' = 0.0602$. Because the overall model is the sum of the two processes, the overall termination point for the *Δu′* component of chromaticity shift was determined to be $\Delta u' = 0.0564$. The *Δv′* component of chromaticity shift also increased during the second, slower process, and it was fit with a logistic model. The termination point for the second process of chromaticity shift for the *v′*

coordinate was also unable to be determined before device failure, but the model suggests a termination point for the second chromaticity shift to be $\Delta v' = 0.111$, making the overall termination point for the $\Delta v'$ component of chromaticity shift to be $\Delta v' = 0.107$.

One logistic function and one bounded exponential function were added together to optimize the $\Delta u'$ and $\Delta v'$ chromaticity shift models. The optimization was performed with the SSE and least squares methods, and the resulting correlation coefficient (R^2) was high. The statistical parameters are presented in **Table 4-3**. The Durbin–Watson (DW) statistic was calculated for the fits and no autocorrelation was found: for 15 chromaticity coordinates (i.e., 15 observations) and 1 regressor, DW>1.07 implies no autocorrelation [23].

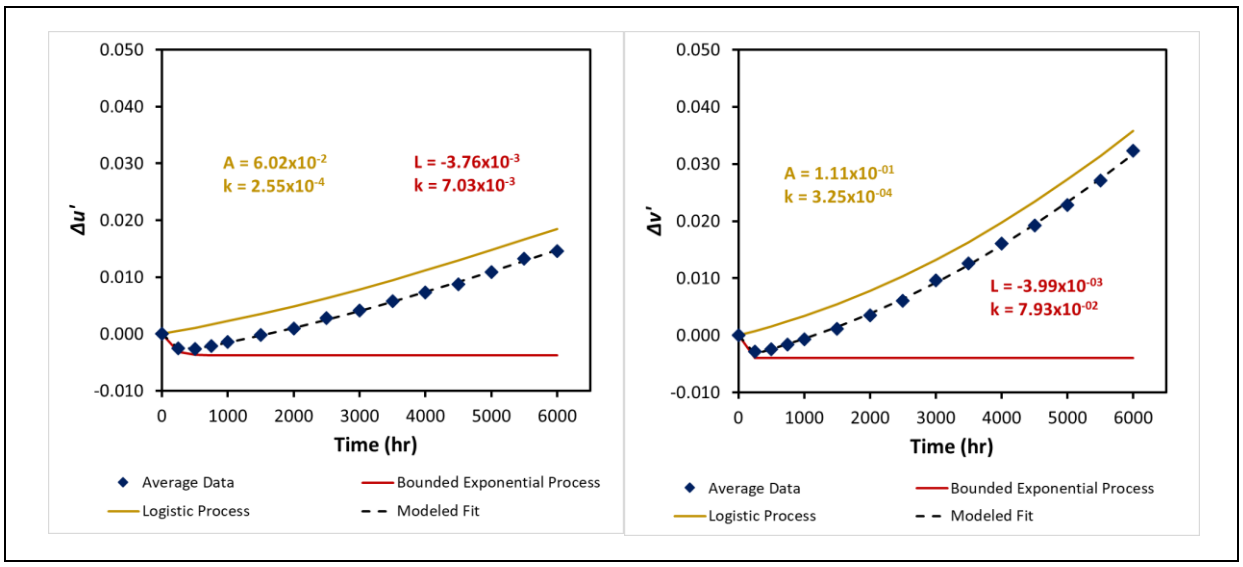

Figure 4-8. Chromaticity shift modeling for the average change in $\Delta u'$ (left) and $\Delta v'$ (right) for the MULTI-H1 DUTs.

Table 4-3. Statistic parameters of models for $\Delta u'$ and $\Delta v'$ for the Multi-H1 DUTs.

$\Delta u'$ Model	
Bounded exponential process	$\Delta u' = (-3.76 \times 10^{-3})\left(1 - e^{-(7.03 \times 10^{-3})t}\right)$
Logistic process	$\Delta u' = -9.54 \times 10^{-3} + \frac{(6.02 \times 10^{-2})}{\left(1 + 5.30e^{-(2.55 \times 10^{-4})(t)}\right)}$
SSE	4.14×10^{-7}
R^2	0.999
DW statistic	2.26
$\Delta v'$ Model	
Bounded exponential process	$\Delta v' = (-3.99 \times 10^{-3})\left(1 - e^{-(7.93 \times 10^{-2})t}\right)$
Logistic process	$\Delta v' = -1.02 \times 10^{-2} + \frac{(1.11 \times 10^{-1})}{\left(1 + 9.90e^{-(3.25 \times 10^{-4})(t)}\right)}$
SSE	1.54×10^{-6}
R^2	0.999
DW statistic	1.39

In a previous report [8], the chromaticity shift of the six MULTI-H2 samples was detailed through 3,000 hrs. In summary, $\Delta u'$ shifted in the positive direction, and $\Delta v'$ shifted in the negative direction within the first 250

hrs. Subsequently, a period of minimal chromaticity shift was observed, particularly in the $\Delta v'$ coordinate. At an emergence time of 4,000 hrs, the dominant chromaticity shift started, wherein both $\Delta u'$ and $\Delta v'$ coordinates shifted in the positive direction, as shown in Figure 4-7. The positive chromaticity shift continued until either the DUT failed (parametrically or "lights out") or until the DUTs were removed from testing at 8,000 hrs.

The temporal behaviors of the $\Delta u'$ and $\Delta v'$ coordinates for the MULTI-H2 DUTs are shown in **Figure 4-9**. The $\Delta u'$ component of chromaticity shifted quickly (<1,000 hrs) in a positive direction, and then plateaued. The bounded exponential model of the initial process involved in the $\Delta u'$ component of chromaticity shift was updated to reflect a higher asymptotic limit of $\Delta u' = +0.0066$ (Figure 4-9, see image on left). After the initial bounded exponential process, the $\Delta u'$ component of chromaticity experienced an induction period (until approximately 3,500 hrs) before continuing to shift in a positive direction through the end of testing (8,000 hrs or device failure). A logistic model was used to fit the incubated process that shifted the $\Delta u'$ component in a positive direction starting at approximately 3,500 hrs. Testing was terminated at 8,000 hrs (to allow for additional testing after three out of the six of the devices failed); therefore, an exact termination point for the second chromaticity shift modeled by the logistic function could not be determined, although the current model suggests $\Delta u' = 0.0582$. Therefore, the overall chromaticity shift, which is modeled as the sum of the bounded exponential process and the logistic process, has an estimated terminal chromaticity shift of $\Delta u' = +0.0648$.

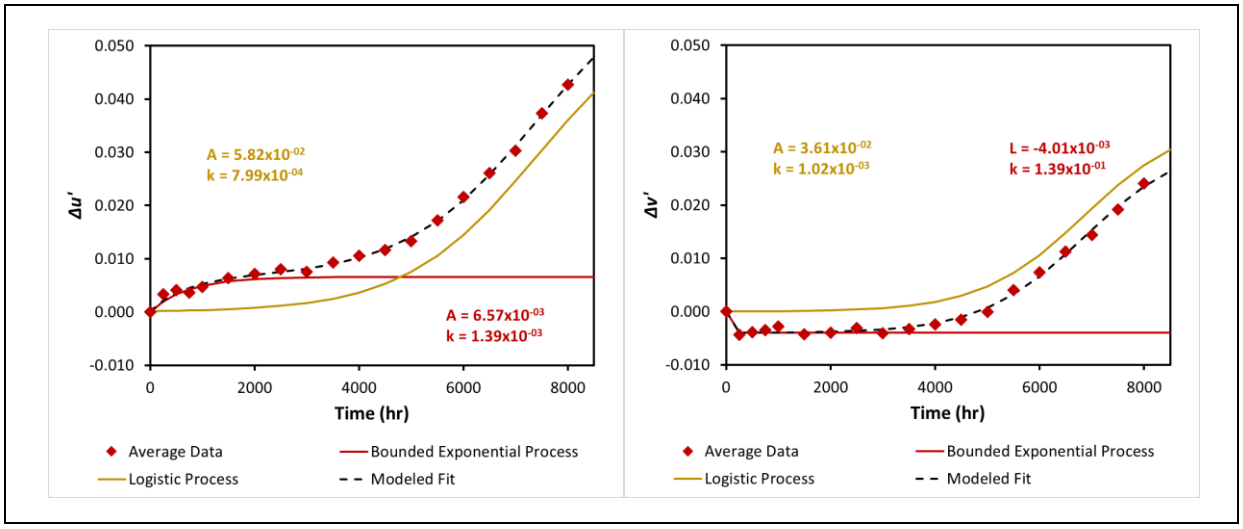

Figure 4-9. Chromaticity shift modeling for the average change in $\Delta u'$ (left) and $\Delta v'$ (right) for the MULTI-H2 DUTs.

A big, initial shift was also observed for the $\Delta v'$ component of chromaticity shift for the MULTI-H2 DUTs. The negative shift was complete within the first 250 hrs of exposure, wherein $\Delta v'$ dropped to a lower asymptotic limit (L) of $\Delta v' = -0.0040$. After the initial chromaticity shift, the $\Delta v'$ component of chromaticity shift remained at the lower asymptotic limit until approximately 3,500 hrs. Upon completion of the incubation period, the $\Delta v'$ component of chromaticity shifted to positive values. The positive shift was fit with a logistic function and, although testing was terminated before an upper asymptote could be detected, the model suggests $\Delta v' = 0.0361$, yielding an overall approximate termination point of $\Delta v' = +0.0321$.

The chromaticity shift models of $\Delta u'$ and $\Delta v'$ were optimized by summing one logistic function and one bounded exponential function. The statistical parameters are presented in **Table 4-4**. The correlation coefficient (R^2) was high for the fits, and the DW statistic confirmed minimal autocorrelation of the residuals.

Table 4-4. Statistic parameters of models for $\Delta u'$ and $\Delta v'$ for the MULTI-H2 DUTs.

$\Delta u'$ Model	
Bounded exponential component	$\Delta u' = (6.57 \times 10^{-3})\left(1 - e^{-(1.39 \times 10^{-3})t}\right)$
Logistic component	$\Delta u' = \frac{(5.82 \times 10^{-2})}{\left(1 + 7.31e^{-(7.99 \times 10^{-4})(t - 4900)}\right)}$
SSE	5.94×10^{-6}
R^2	0.999
DW statistic	2.02
$\Delta v'$ Model	
Bounded exponential component	$\Delta u' = (-4.01 \times 10^{-3})\left(1 - e^{-(1.39 \times 10^{-1})t}\right)$
Logistic component	$\Delta v' = -4.15 \times 10^{-5} + \frac{(3.61 \times 10^{-2})}{\left(1 + 10.74e^{-(1.02 \times 10^{-3})(t - 4524.9)}\right)}$
SSE	6.97×10^{-6}
R^2	0.997
DW statistic	1.70

4.5 Changes in Lenses

Thorough descriptions of the lenses used in the products examined in this current study were provided in the previous Round 1 report [8]. For completeness, a summary of the shape and function of the lenses is provided here. The lenses of the two horticulture products examined in this study are significantly different, with the light from individual LEDs being directed to individual lenses in the MULTI-H2 product and to multiple concentric lenses in the MULTI-H1 product. Specifically, the MULTI-H1 PAR38 grow lamp uses one large lens that consists of multiple concentric, concave lenses, with the innermost lens being a centrally located dome-like structure approximately 1.7 inches in diameter that diverges the light produced by the LED module. The outer concentric lenses of this structure are faceted to provide additional light divergent capability. Together, the structure of concentric lenses that form the lens in MULTI-H1 devices helps to diverge the LED light produced by a cluster of 20 LED packages away from the center of the LED module. The MULTI-H2 PAR38 grow lamps use a single lens consisting of 16 separate concave lenses to shape light above each of the 16 LED packages. Each of the 16 concave lenses is placed over one MP-LED package and receives light only from that LED. The diameter of each of the 16 concave lenses is approximately 0.56 inches on the top surface. The lenses of both the MULTI-H1 and MULTI-H2 products are molded from PC resin.

In the Round 1 report, evidence of photo-oxidation (lens yellowing) and thermomechanical stress (hairline cracking) was seen in the lenses from MULTI-H1 DUTs, but only photo-oxidation was observed in the MULTI-H2 lenses [8]. The secondary lenses on the MULTI-H1 DUTs did not appear to experience additional hairline cracks after 3,000 hrs of testing. However, as the DUTs continued to age, the PC lenses became increasingly more yellow for both products. This behavior also agrees with findings in the scientific literature [24]. The aged lenses are shown in **Figure 4-10** and **Figure 4-11** after 6,500 hrs (directly after abrupt device failure) for the MULTI-H1 DUTs and after 8,000 hrs (after testing suspension) for the MULTI-H2 DUTs.

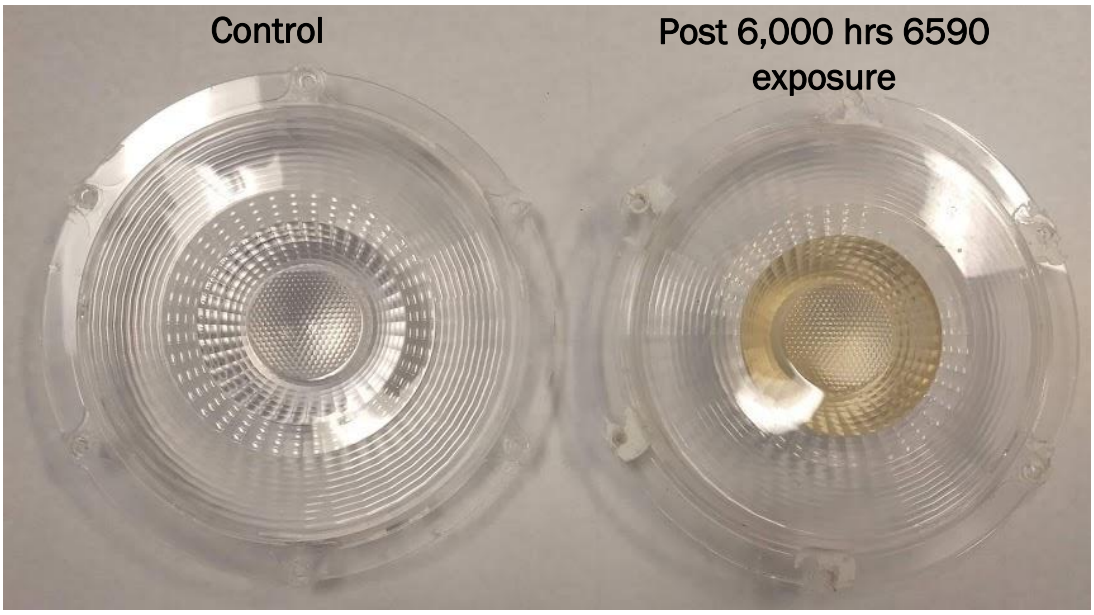

Figure 4-10. Aged lenses of the MULTI-H1 DUTs are yellowed (right), especially in the center region, compared to the control (left).

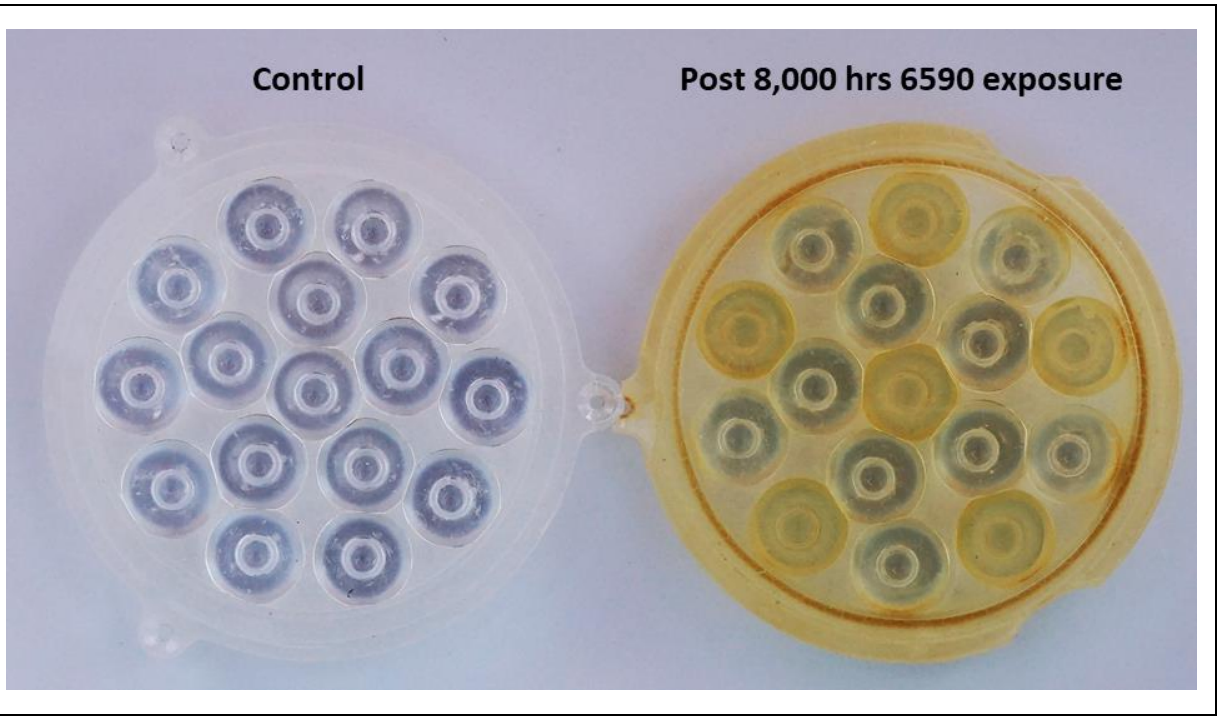

Figure 4-11. A comparison of a control lens (left) and an aged lens (right) for the MULTI-H2 DUTs. The aged lens shows that pcLEDs accelerate lens yellowing relative to the red LEDs in the MULTI-H2 DUTs.

The MULTI-H1 DUTs visibly showed more lens yellowing in the concave lens of the central dome region (directly above the location of the pcLEDs used in this device) relative to the outer region of concentric lenses. The diffuse transmittances of these two regions were recorded for two samples that abruptly failed at approximately the same time (approximately 6,100 hrs) and compared with the control sample as shown in

Figure 4-12. The diffuse transmittances of both regions decreased in the aged samples, with the diffuse transmittance of the concave inner lens region decreasing more than the outer region. Because it is known that blue light accelerates photo-oxidation of PC materials [24], increased yellowing in the central region of the lens where radiant energy is highest supports the idea that photo-oxidation accelerated by the heat and humidity of the 6590 environment is likely the primary cause of yellowing in these lenses. It should be noted that the reported diffuse transmittances in both regions are subject to experimental constraints, given the size and curved surfaces of the lenses, and may not reflect the absolute magnitude of the diffuse transmittances of the lens because the entire lens can only be sampled with the UV-Vis spectrometer in a few regions and angles of incidence. As a result, the transmittance of outer region of the lens could be readily measured with the UV-Vis spectrometer, whereas the transmittance of the inner region of the lens could only be measured in a modified setup (see **Section 2**). Finally, it should be noted that the magnitude of lens yellowing was different between the two aged samples even though they started with similar radiant fluxes (4.201 W versus 4.14 W), and aging time was approximately the same (approximately 6,100 hrs). The difference in magnitude of lens yellowing could be caused by variations in light-focusing capability between lenses and reflectors, differences in pcLED degradation rates between the two samples, or other factors that might cause the sample with lower lens transmittance (DUT 411) to operate at a higher temperature. Variability in operating temperature and increasing operating temperature with aging were described in our previous report [8].

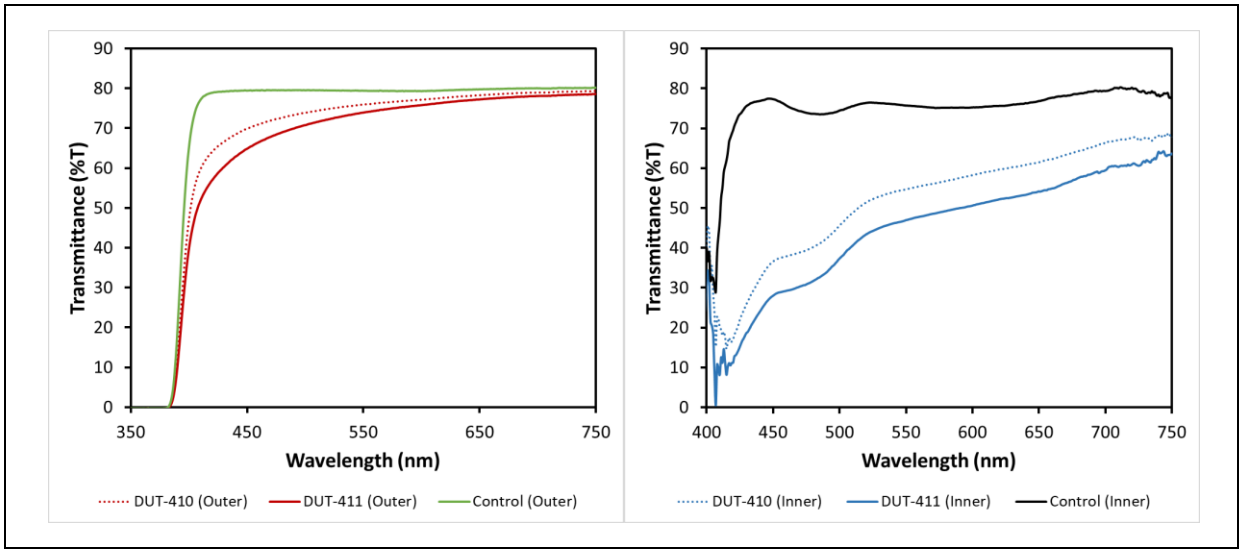

Figure 4-12. Diffuse transmittance spectra of the MULTI-H1 lenses show different rates of aging based upon whether transmittance is measured for the outer region of the lens (left) or the inner central concave lens region (right).

The lenses of the MULTI-H2 DUTs also continued to yellow with time, and no signs of cracking were observed. The individual concave lens responsible for shaping light above the individual LED packages yellowed at two different rates, with the lens on top of the pcLEDs turning a deeper yellow than the lens on top of the red-emitting LEDs (Figure 4-11). The diffuse transmittances of the lenses in these two regions were recorded for two DUTs using the UV-Vis spectrometer after 8,000 hrs of exposure and compared with the control as shown in **Figure 4-13**. Unlike the MULTI-H1 DUTs, the diffuse transmittances of the lenses on top of the pcLEDs were similar for the two aged MULTI-H2 DUTs: DUT 376 and DUT 377. Similarly, the diffuse transmittances of the lenses on top of the red LEDs were similar for the two aged MULTI-H2 DUTs. The uniformity in aging among red lenses and blue lenses suggests that each lens aged consistently and extracted light efficiently, minimizing breaches of blue-enriched light into the areas of red-light emission. In this way, wavelength-dependent photo-oxidation effects of the PC resin were isolated in the MULTI-H2 DUTs but not in the MULTI-H1 DUTs.

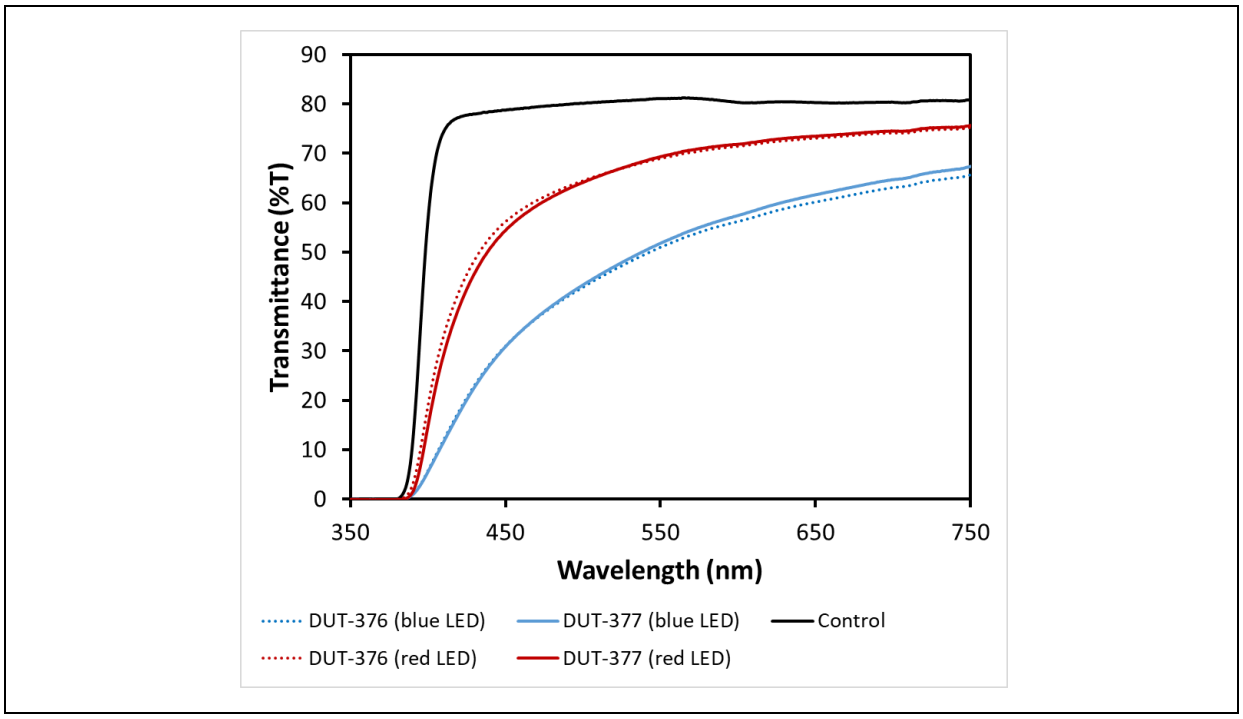

Figure 4-13. Diffuse transmittance spectra of the dome-like structures of the MULTI-H2 lenses show different rates of aging based upon whether the dome is spatially located to focus blue-enriched light from the pcLED or red-enriched light from the red LED. The transmittance spectra of two DUTs are shown and compared with a control sample, which was not operated.

To better understand the effects of the yellowed lenses on radiant flux maintenance and chromaticity shift, the SPDs of a representative lamp are shown prior to operation (0 hrs) and at the end of testing (see **Figure 4-14** for MULTI-H1 and **Figure 4-15** for MULTI-H2). Because all MULTI-H1 DUTs experienced abrupt failure, a representative SPD was obtained by replacing the LED module of the control lamp with the LED module of DUT-410. In this way, the electrical driver of the control lamp supplied power to the LED module of DUT-410, and the lens of DUT-410 was placed over the LED module of DUT-410 to understand lens effects on radiant flux and chromaticity shift. Prior to device failure, radiant power in the blue region (400–500 nm) for DUT 410 was approximately half (52%) of its original value, whereas radiant power in the red region only decreased to approximately 71% of its original value. After the lens was removed, most of the radiant flux in the blue region was regained (radiant power was 78% of its original value). In contrast, only a small portion of the radiant flux was regained in the red region (radiant power was 72–73% of its original value, see Figure 4-14). It should be noted that these radiant power data are approximations because the original driver and lamp configuration could not be tested for the MULTI-H1 DUTs. The power consumed by the control lamp with DUT-410's LED module was similar to the power consumed directly by the DUT before device failure, and therefore a good approximation for the true SPD if device failure had not occurred. These data support lens yellowing and filtering of blue light as the major contributor to the proportionately greater loss of blue light.

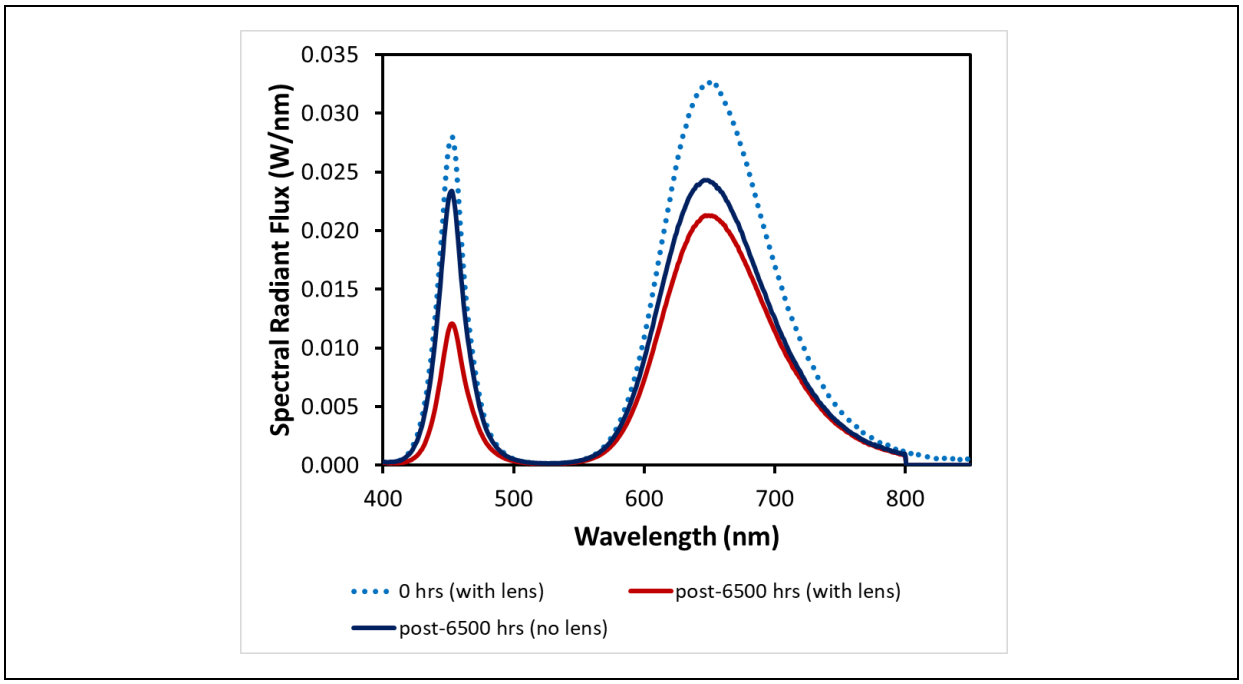

Figure 4-14. Measured SPDs of a MULTI-H1 lamp (DUT-410) prior to AST exposure and post-6,500 hrs* of exposure to 6590 before and after the lens was removed demonstrate the impact of lens yellowing on blue emissions. (* The LED module of DUT-410 was attached to the driver of the control lamp to accommodate this test.)

The SPDs of the MULTI-H2 DUTs were spectrally deconvoluted into individual emitter components and the radiant power for each emitter is summarized in **Table 4-5**. To perform the spectral deconvolution for the phosphor and direct LED emissions, each emitter was modeled with a separate function to estimate individual emitter contributions (radiant power) to the overall SPD. The blue LED was modeled with a logistic power peak function. The green phosphor was modeled with two skewed Gaussian distributions because its broad emission wavelength was consistent with YAG:Ce, which experiences two 4f → 5d electronic transitions. The red LED was modeled with a split function (logistic power peak when the wavelength (p) was less than the peak wavelength (p_o) and a second order Lorentzian when $p > p_o$). The radiant powers calculated in **Table 4-5** are the average radiant power derived from the SPDs of the operational MULTI-H2 DUTs at the respective time point. The total lamp system attenuation (Equation 1) describes the total radiant power lost for the lamp system, which includes lens losses, LED degradation losses, and LED module/package effects. The spectral deconvolution after 8,000 hrs of exposure to 6590 shows that the total lamp system attenuation was greatest at blue and green wavelengths, and minimum radiant power attenuation was observed at the longer, red wavelengths.

To separate the LED degradation and LED module/package radiant power attenuation from the lens attenuation, the original aged lens was replaced with a control lens and the SPD was measured. The SPDs of the unaged sample (0 hrs [with lens]), aged sample (8,000 hrs [with original aged lens]), and aged sample with control lens (8,000 hrs [control lens]) were then compared and used to calculate the radiant power attenuation of the lens relative to the radiant power attenuation attributed to the total lamp system (represented as the Lens Contribution Attenuation, Equation 2). The SPDs and associated spectral modeling indicate that when the lenses of the MULTI-H2 devices were removed and replaced with a control lens, the blue emission peak shifted back toward its original peak position and the measured amplitude was similar to the original amplitude of a lamp with the lens in place (Figure 4-15). The lens significantly impacted the blue-emitter attenuation, accounting for 83.2% of the total blue-emitter attenuation. The green and red emission peaks also recovered some of their initial amplitude, albeit at lower magnitudes. The radiant fluxes from phosphor and red LED

emissions were not as affected by lens yellowing (30.1% and 40.0% loss of the total radiant flux attenuation, respectively, compared to their initial values). Equations 1 and 2 are presented as follows:

$$Total\ Lamp\ System\ Attenuation = Radiant\ Power_{0\ hrs\ (with\ lens)} - Radiant\ Power_{8{,}000\ hrs\ (aged\ lens)} \quad \text{(Eq. 1)}$$

$$Lens\ Contribution\ Attenuation = \frac{Radiant\ Power_{8{,}000\ hrs\ (control\ lens)} - Radiant\ Power_{8{,}000\ hrs\ (aged\ lens)}}{Radiant\ Power_{0\ hrs\ (with\ lens)} - Radiant\ Power_{8{,}000\ hrs\ (aged\ lens)}} \times 100 \quad \text{(Eq. 2)}$$

From these data, it is clear that the phosphor was the least stable light-emitting component on the MULTI-H2 DUTs, and the lens was primarily responsible for approximately 83% of the blue emission loss through filtering.

Table 4-5. Average radiant power attenuation attributed to the MULTI-H2 lenses.

	Radiant Power (W)				Lens Contribution Attenuation (% of original value)
	0 Hrs	8,000 Hrs (Aged Lens)	8,000 Hrs (Control Lens)	Total Lamp System Attenuation	
Blue-emitting LED	0.785 ± 0.001	0.322 ± 0.030	0.708 ± 0.017	0.463 ± 0.030	83.2 ± 4.7
Phosphor	1.601 ± 0.017	0.919 ± 0.053	1.123 ± 0.057	0.682 ± 0.053	30.1 ± 3.0
Red-emitting LED	2.140 ± 0.017	1.950 ± 0.041	2.030 ± 0.016	0.189 ± 0.046	40.0 ± 19.4

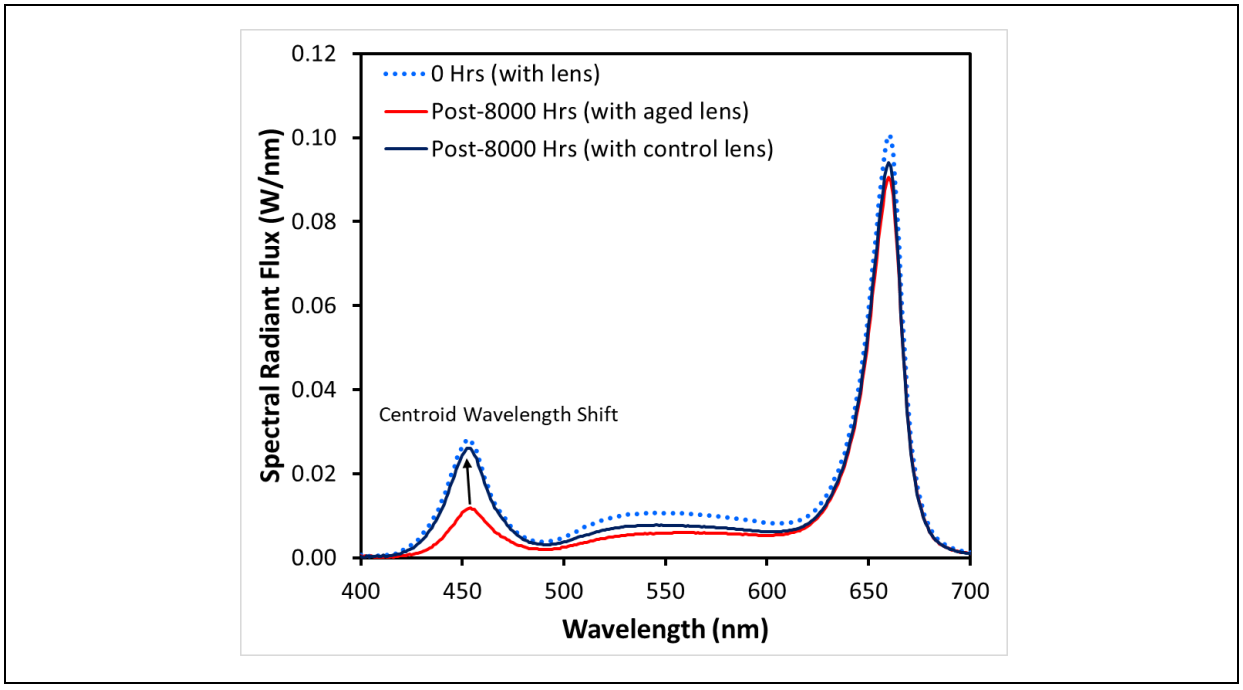

Figure 4-15. Measured SPDs of a MULTI-H2 DUT post-8,000 exposure to 6590 before and after the lens was removed demonstrate the impact of lens yellowing on blue emissions.

The impacts of these spectral changes on chromaticity of the devices were significant. For the MULTI-H1 DUT, the chromaticity coordinates of both *u′* and *v′* shifted in a positive direction over device operation while the lens was attached. However, after the lens of DUT 410 was removed, the *u′* and *v′* values were less than the pre-exposure chromaticity coordinates as shown in **Figure 4-16**. The shift to lower *u′* and *v′* chromaticity coordinates is likely the consequence of a faster rate of red phosphor degradation relative to blue LED degradation observed for the MULTI-H1DUTs (Figure 4-3). For the MULTI-H2 DUT, the *u′* component of chromaticity shift was increased with the aged lenses and after replacing the aged lens with the control lens, whereas the *v′* component of chromaticity shift was increased with the aged lenses and decreased when the aged lens was replaced with the control lens (**Figure 4-17**). The positive shift in *u′* was a combination of lens filtering of blue and green wavelengths and increased stability of the red LED relative to the phosphor. In general, changes in the *u′* direction are strongly influenced by changes in the ratio of green to red emissions in the emitted light, whereas changes in the *v′* direction are more affected by the ratio of blue to yellow emissions. Specifically, *u′* shifted to a larger value when the aged lens was attached because the lens filtered out a larger portion of green light relative to red; however, when the aged lens was removed and replaced with the control lens, a smaller shift in the positive direction for the *u′* value was observed due to a restoration of the green emissions filtered by the lens. Similarly, the shift in *v′* was a combination of lens filtering of blue emissions and increased stability of the blue LED relative to the phosphor which is the source of yellow emissions. The increase in *v′* (for aged lenses) was due to the lens filtering out blue emissions at a higher proportion than filtering of green and yellow emissions. The decrease in *v′* (after the aged lens is replaced with the control lens) resulted from proportionately more blue than yellow emissions passing unfiltered through the lens due to the greater stability of the blue LED relative to the phosphor.

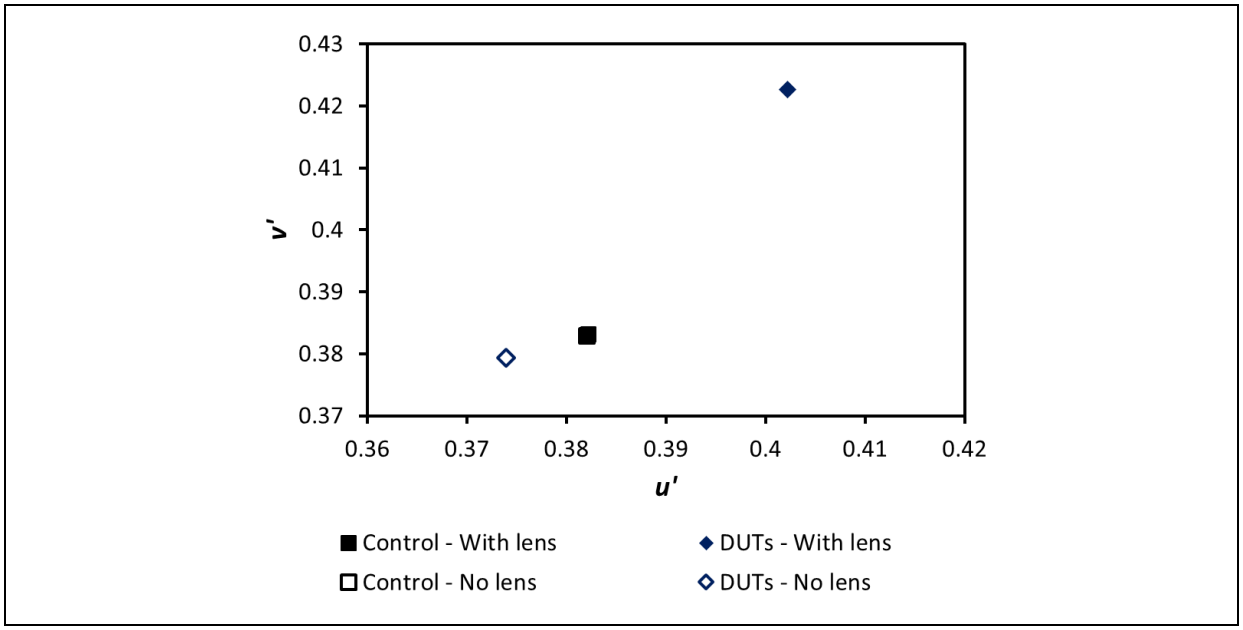

Figure 4-16. Chromaticity coordinates of the MULTI-H1 control and chromaticity coordinates of DUT-410 post-6,500 hrs of exposure to a 6590 environment with and without the lens attached. The chromaticity coordinates of DUT-410 prior to exposure were within experimental error of the control chromaticity coordinates (not shown), and the control chromaticity coordinates with and without the lens attached overlap.

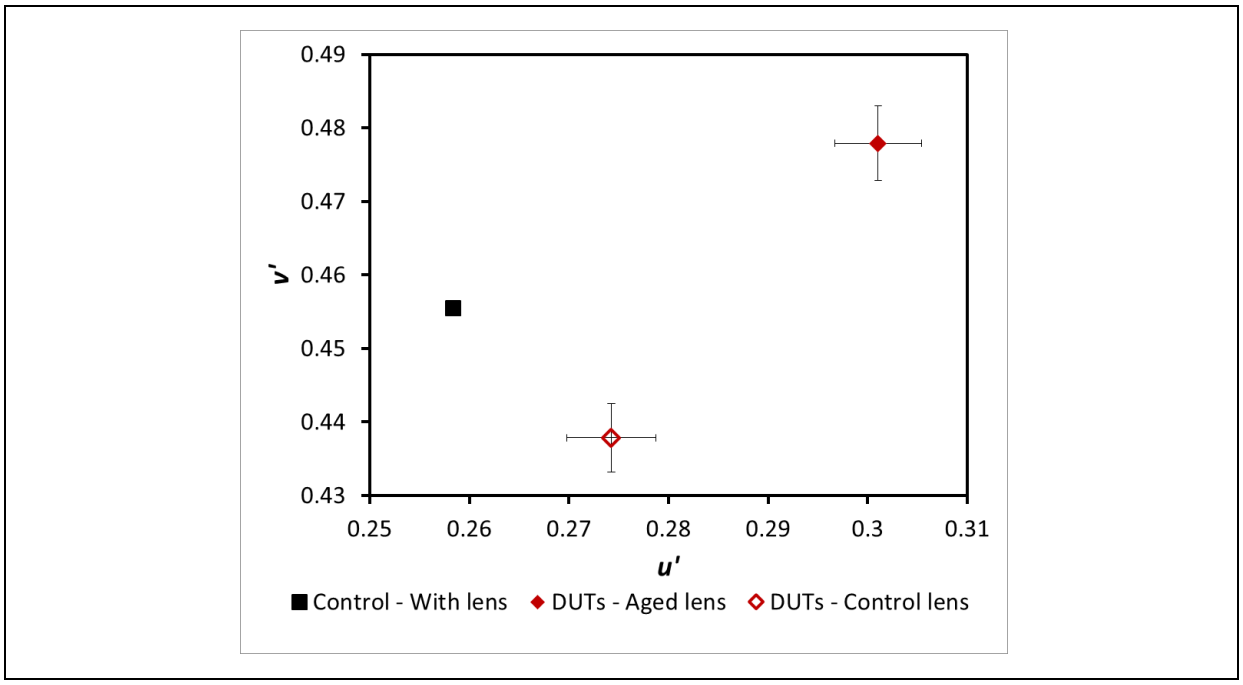

Figure 4-17. Chromaticity coordinates of the MULTI-H2 control and average chromaticity coordinates of the MULTI-H2 DUTs post-8,000 hrs of exposure to a 6590 environment with aged lenses and a control lens attached. The average chromaticity coordinates of the MULTI-H2 DUTs prior to exposure were within experimental error of the control chromaticity coordinates (not shown).

4.6 Component Analysis

This section of the report discusses the components that led to failure for the MULTI-H1 and MULTI-H2 DUTs. For the DUTs that did not fail, a component analysis was performed to check functionality compared with a control device. Because **Section 4.5** discussed lens yellowing, the lenses of the devices are not discussed in this section.

By the end of 6,500 hrs of 6590 exposure, all six MULTI-H1 DUTs failed, and by the end of 8,000 hrs of 6590 exposure, three out of the six MULTI-H2 DUTs failed (**Table 4-2**). When the devices were disassembled, signs of aging were immediately observed on the LED modules: the MULTI-H1 modules were ashy and cracked, and the MULTI-H2 modules were a brownish color, with darker shades of brown surrounding the red LEDs (**Figure 4-18**).

The ashy color and cracking of the LED modules from the MULTI-H1 DUTs were centered around the LEDs in a circular shape, and the diameter of the circle was consistent with the diameter of the hole in the reflector that was situated over the center of the LEDs. The reflector was discolored in the direction of the primary lens, but it was not discolored as much on the opposite side. The one-sided discoloration of the reflector was previously observed in AST studies on other LED products and is likely an indication of a photo-activated process of degradation [25]. For the MULTI-H2 modules, the circular area around the pcLEDs was whiter (but not light blue) than the remainder of the LED module, suggestive of an influence from the lens. The LED packages showed signs of aging (e.g., discoloration of the package molding resin) that was especially prevalent for the red LEDs.

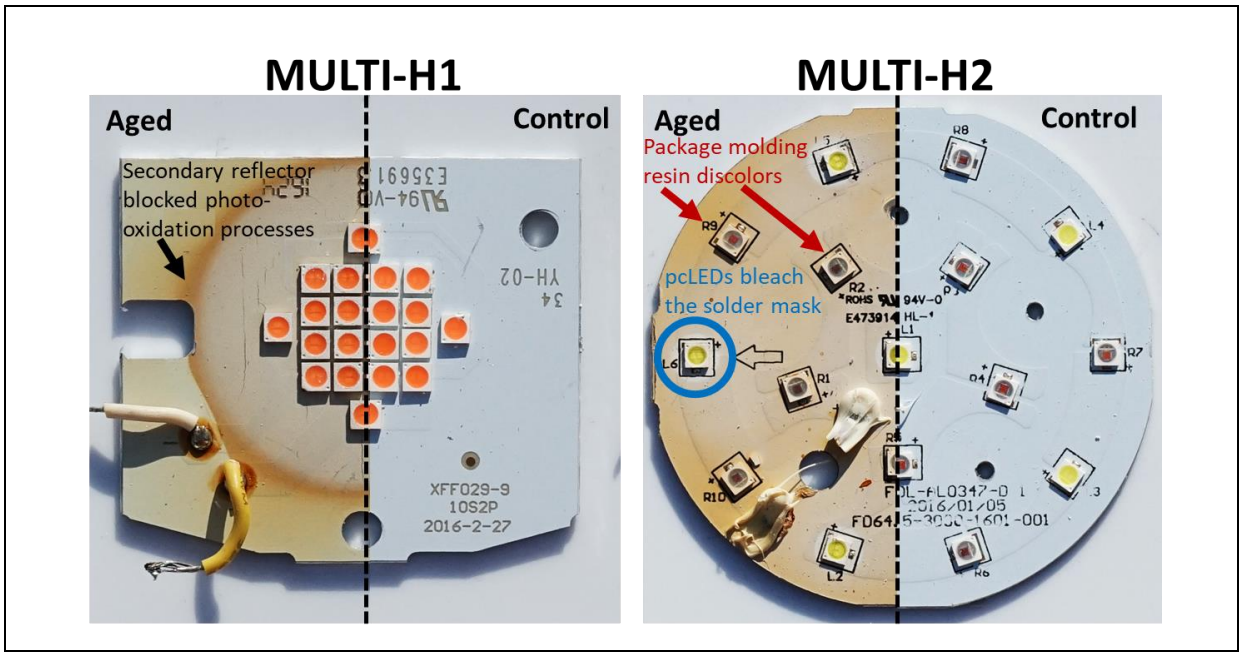

Figure 4-18. The aged LED modules of the MULTI-H1 devices post-6,500 hrs (left) and MULTI-H2 devices post-8,000 hrs (right) of aging in the 6590 environment show various levels of discoloration, cracking, and photo-oxidation compared to their controls.

Visual inspections of the electrical drivers of the MULTI-H1 DUTs revealed apparent fuse failures: the fuses were either blackened, brittle, or both, and they often snapped in half during disassembly. An electrical analysis revealed that abrupt failure of the drivers was the root cause of failure for five out of the six DUTs. Those five DUTs experienced a cascade of failures involving the fuse, diode bridge, isolation transformer, and MOSFET components. In the sixth device, two LED packages failed (they appeared carbonized [**Figure 4-19**]), the fuse blew, and a capacitor in the electromagnetic interference (EMI) filtering stage was blown (but the capacitor still functioned [**Figure 4-20**]). Although it cannot be completely determined whether the LED packages failed before or after the capacitor, because the capacitor still had functionality, the LED module was listed as the cause of the abrupt failure of this DUT.

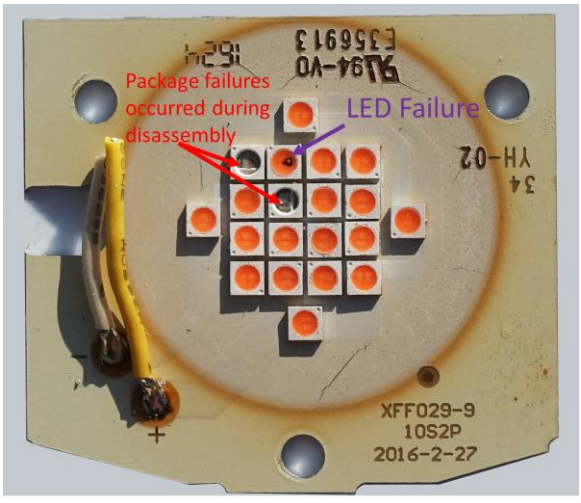

Figure 4-19. DUT-411, a MULTI-H1 device, experienced abrupt failure on the LED module.

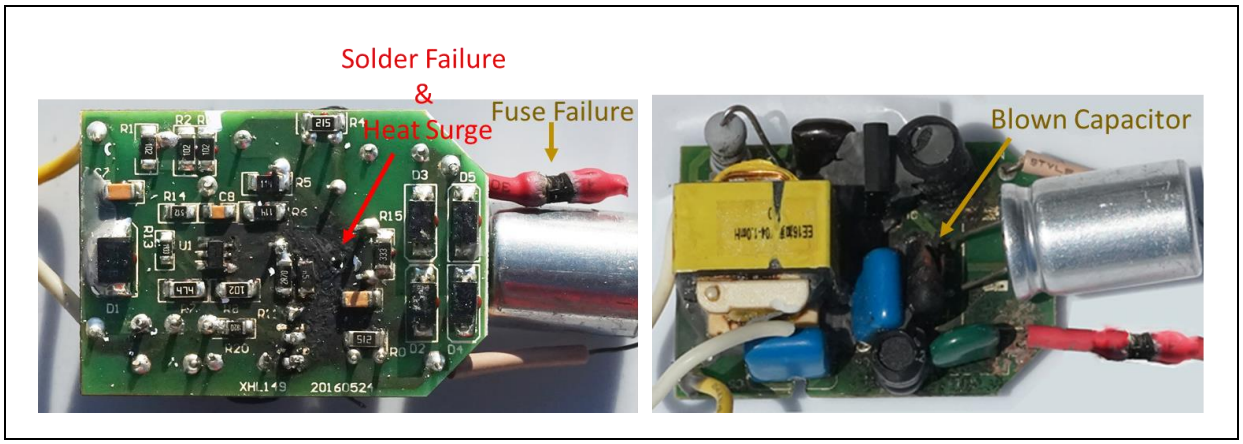

Figure 4-20. The bottom of the driver for DUT-411, a MULTI-H1 device, showed evidence of solder failure, heat surge and fuse failure (left) and the top of the driver housed the blown, but functioning, capacitor (right)

The electrical drivers of the MULTI-H2 DUTs were also darker than the control sample, with a localized dark patch on part of the board beneath the transformer. Some of the conductive tracks between electronic components were also dark, particularly near the alternating current mains input and between the diode bridge and transformer pins. The dark areas on the PCB indicate high-stress areas where temperature is high. These areas can be used to identify areas subject to copper delamination from the PCB due to excessive humidity and/or heat. The two MULTI-H2 parametric failures were caused by lens yellowing and subsequent blue light filtering by the lenses as described in **Section 4.5**. The drivers of the MULTI-H2 DUTs that experienced parametric failure and the drivers of the DUTs that were right censored experienced minimal change relative to the control driver at the end of testing. The sixth MULTI-H2 DUT experienced an abrupt failure on the LED driver because of multiple failures: the diode bridge failed, capacitor C2 erupted (C2 was part of the EMI filter), the conductive track near the erupted C2 capacitor delaminated from the PCB and cracked in half, three resistors and one capacitor near the transformer experienced solder failure, and the fuse was open. These failures are shown in **Figure 4-21**.

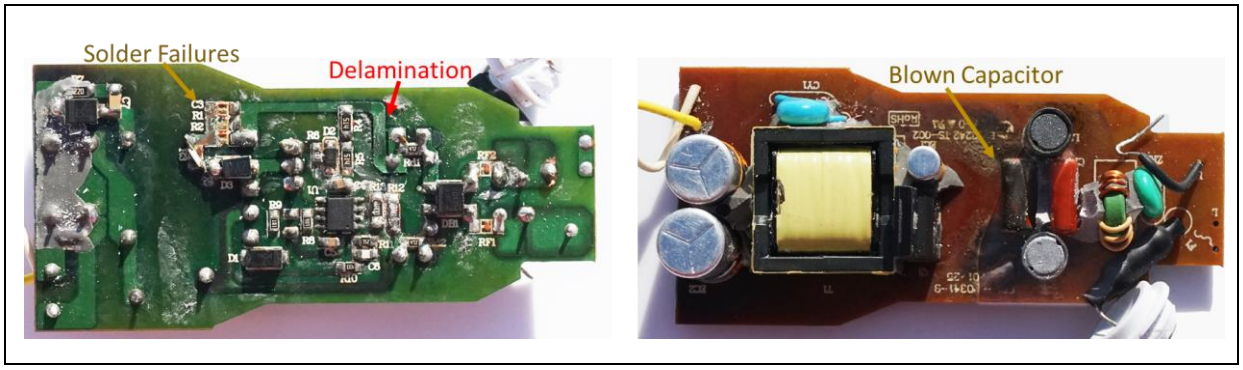

Figure 4-21. DUT 401, an MULTI-H2 driver, post-8,000 hrs of aging in 6590 underwent solder failures of three components, delamination and discoloration of the PCB and its conductive track (left), and an EMI capacitor blew (right).

5 Discussion

The relatively small size and high luminance of LEDs provide the flexibility to produce SSL devices that incorporate many LED packages of varying size, luminous flux emissions, chromaticity, and other properties. The ability to integrate multiple LEDs with different characteristics into a single device to create multi-source LED products provides an enhanced functionality in SSL devices that is difficult—if not impossible—to achieve with conventional lighting technologies. These multi-source LED devices can have a fixed

chromaticity or, if appropriate driver electronics are included, the light emissions can be tuned by adjusting the current supplied to each LED primary. Although multi-source LEDs are creating new markets for SSL technologies, this current study demonstrates that the aging properties of such devices can vary widely, depending on the device architecture and the properties of the LED primaries. These aging differences can have significant impacts on the quality of light, including changes of the luminous flux levels, chromaticity, and tuning range beyond what occurs for fixed-CCT devices. Consequently, careful consideration must be given to potential aging differences in the LED primaries and their long-term impacts on all components of an SSL device. As shown in **Figure 5-1**, the impacts of using multiple LED sources must be approached at the system level. The three main system components (i.e., LED packages; device optics, including secondary lenses, reflectors, and housings; and device electronics and controls) impact the long-term performance and reliability of the multi-source LED device to varying degrees.

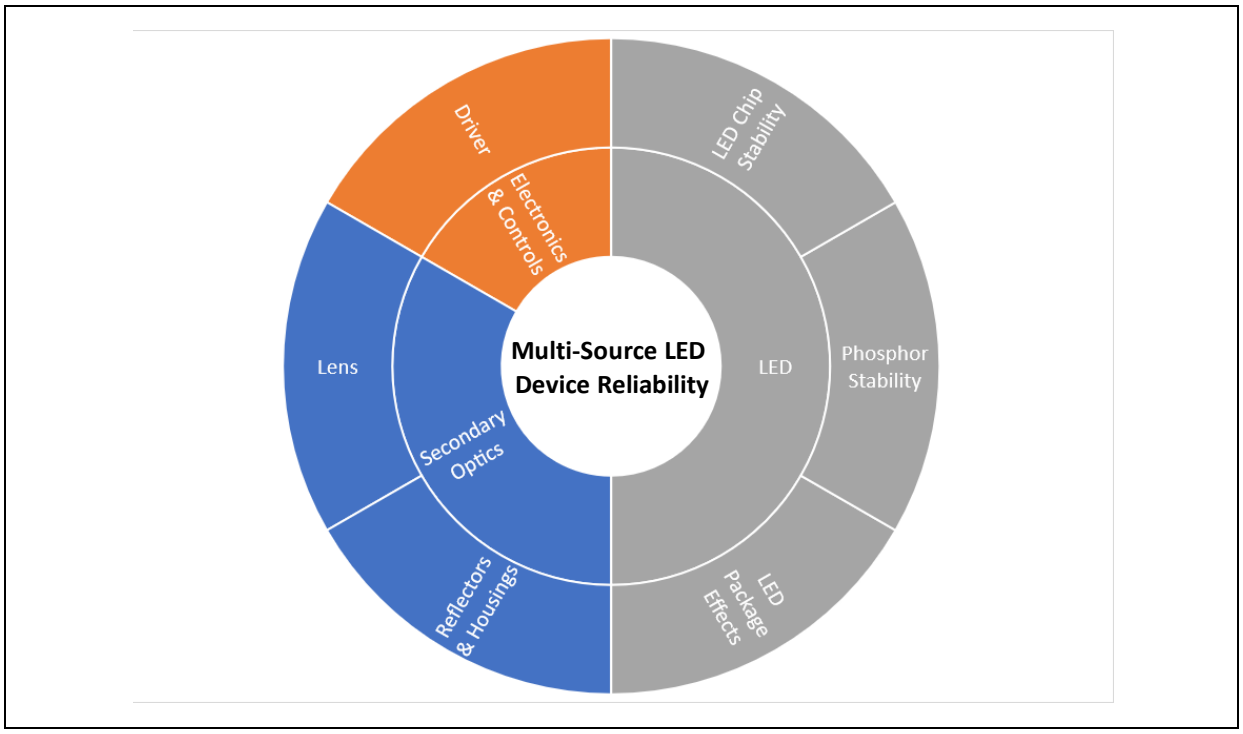

Figure 5-1. Major system components and sub-components affecting the long-term reliability of multi-source LED devices.

Impacts of the LED

The LED component of an SSL device consists of three major sub-components: the LED chip or die, the phosphor (for pcLED devices), and the package. The stability of the LED chip is the foundation of luminous flux and chromaticity performance in any SSL device. An evaluation of LM-80-15 data for some direct emitting high-power LEDs (HP-LEDs) showed that both royal blue (peak wavelength near 450 nm) and red LEDs (peak wavelengths near 620 nm) have excellent stability for both parameters [26]. This analysis examined the HP-LED package because it is generally more stable than the MP-LED package, as judged by the range of decay rate constants for luminous flux [9].

Even though all products in the current study used blue LEDs in a pcLED architecture, the behavior of blue emissions from the pcLEDs provides insights into the performance of the blue LED chip in the DUTs. For example, this study found that there was some reduction in the intensity of blue emissions from the MULTI-WT1 LED primaries; however, these changes were completed by 2,500 hrs for both warm white and cool white LED primaries operating at 95°C (see Figure 3-6 and Figure 3-7). Also, the peak shape of the blue LED emissions did not change. For the horticulture lighting products examined during this study, the red direct-

emitting LEDs in the MULTI-H2 DUTs exhibited only a slight change in radiant flux and no significant change in peak location through 8,000 hrs of 6590. However, blue emissions from both horticulture products exhibited some changes in both luminous flux and peak wavelength. For the MULTI-H2 DUTs, the blue radiant flux exhibited a higher rate of decline after 4,000 hrs of 6590 exposure than before, and an increase in the centroid wavelength of the blue peak, which corresponds to a shift in emission wavelength, occurred after 4,000 hrs. For the MULTI-H1 product, there was an increase in the centroid wavelength of blue emissions starting at 2,500 hrs of 6590 exposure that proceeded at an exponential rate for the remainder of the test (6,000 hrs). As will be discussed in the subsection titled *The Impact of the Secondary Lens*, these changes in blue emissions are not due to changes in the LED chip but rather to the impact of blue radiation on other optical components of the SSL device. Consequently, the current study demonstrates that LED chips housed in MP-LED packages can be relatively stable and unlikely to cause parametric failures through changes in peak position or radiant flux levels, analogous to previous findings for HP-LED packages.

The Impact of the Phosphors

Several different phosphor mixes were included in this study to examine the impacts of this sub-component on the reliability of multi-source LED devices. Changes in the relative emission intensities and peak shapes from the phosphors impacted the luminous flux and chromaticity maintenance behavior of the different pcLED products. Changes in phosphor emission peak shapes are often manifested by changes along the u' axis of the 1976 CIE chromaticity diagram, with changes to lower u' (i.e., $\Delta u' < 0$) values indicating a shift toward the green direction, whereas changes to a higher u' (i.e., $\Delta u' > 0$) values indicate a shift toward the red direction. The MULTI-WT1 LED modules examined during this study consisted of both warm white and cool white LED primaries in MP-LED packages, and each LED primary used a different phosphor. The strong shift in the green direction that was observed for the warm white LED primary (see Figure 3-8) can be attributed to a shift of light emissions from the phosphor to lower wavelengths. This shift was previously observed in warm white phosphors and has been attributed to the oxidation of the doped oxynitride phosphors that are typically found in warm white products [8, 12, 20, 21, 22]. In contrast, the chromaticity shift for the cool white LED primary was mainly along the v' axis, suggesting a minimal change in the shape of the emission spectrum for the phosphors and more of a change in the relative amounts of blue and phosphor radiation produced by the package.

The MULTI-H1 product uses a unique phosphor mix to provide red emissions centered near 664 nm. As shown in Figure 4-4, the centroid wavelength of this phosphor did not shift significantly relative to the control. However, the radiant flux exhibited three different regions of decline. Initially, the radiant flux of the red phosphor in the 6590 environment decreased at a near linear rate during the first 500 hrs of testing, and then decreased slowly from 500 hrs to 3,000 hrs. After this time, there was a sharp drop in radiant flux that appeared to be accelerating (see Figure 4-3). Thus, while the phosphor exhibited minimal change in the emission wavelength, there was a quenching mechanism, likely caused by the combination of moisture and heat in the 6590 environment, that significantly impacted the radiant flux maintenance of the device.

Based on the findings from this work, the phosphors can significantly impact the parametric stability of multi-source LEDs, and the probably of parametric failure caused by the phosphor is low for some phosphors (e.g., YAG:Ce) and higher for other phosphors that are less stable (e.g., some red and warm white phosphors).

The Impact of the LED Package

In general, the packaging materials used in MP-LEDs are known to produce higher decay rate constants for luminous flux than HP-LED packages [9]. The package structure of MP-LEDs can also cause complex chromaticity shift behaviors [12, 13, 14, 22] because the molding resin forms the sidewalls of the LED optical cavity and can become more absorptive with aging, as shown in Figure 5-2. Increased absorption by the polymer resin in the MP-LED package reduces the amount of light that reflects from the side walls and out of the package. Because only photons that are emitted from the LED chip at oblique angles strike the sidewall,

the optical pathway of these photons through the phosphor layer is generally longer than the direct emission path (see Figure 5-2), resulting in more photon conversion by the phosphor. In contrast, photons that do not strike the sidewalls of a MP-LED package but are emitted from the package generally travel through a thinner section of the phosphor layer, resulting in lower photon conversion and higher blue light emission [13, 14]. During initial operation of MP-LED packages light traveling directly through the phosphor combines with light that reflects from the package sidewalls to produce the initial lighting spectrum from the LED; however, as the reflectance of the sidewalls decreases (i.e., absorbance increases), the pathway involving oblique emission of blue photons contributes proportionately less to the total light output and the light emissions become progressively enriched in blue. This analysis suggests that the decrease in reflectance of the sidewalls is responsible for the large blue shift observed in the cool white LED primary on the MULTI-WT1 LED modules (see Figure 3-8). This finding is also supported by the discoloration and cracking of the MP-LED packages for the cool white LED primaries (see Figure 3-3). Ironically, neither this CSM nor evidence of package cracking was found for the warm white LED primaries, even though they were located beside the cool white primaries and underwent the same test conditions. We attribute this difference to the higher phosphor loading of the warm white package, which converted a greater percentage of blue photons as they are emitted from the LED chip and reduced the severity of the sidewall aging process.

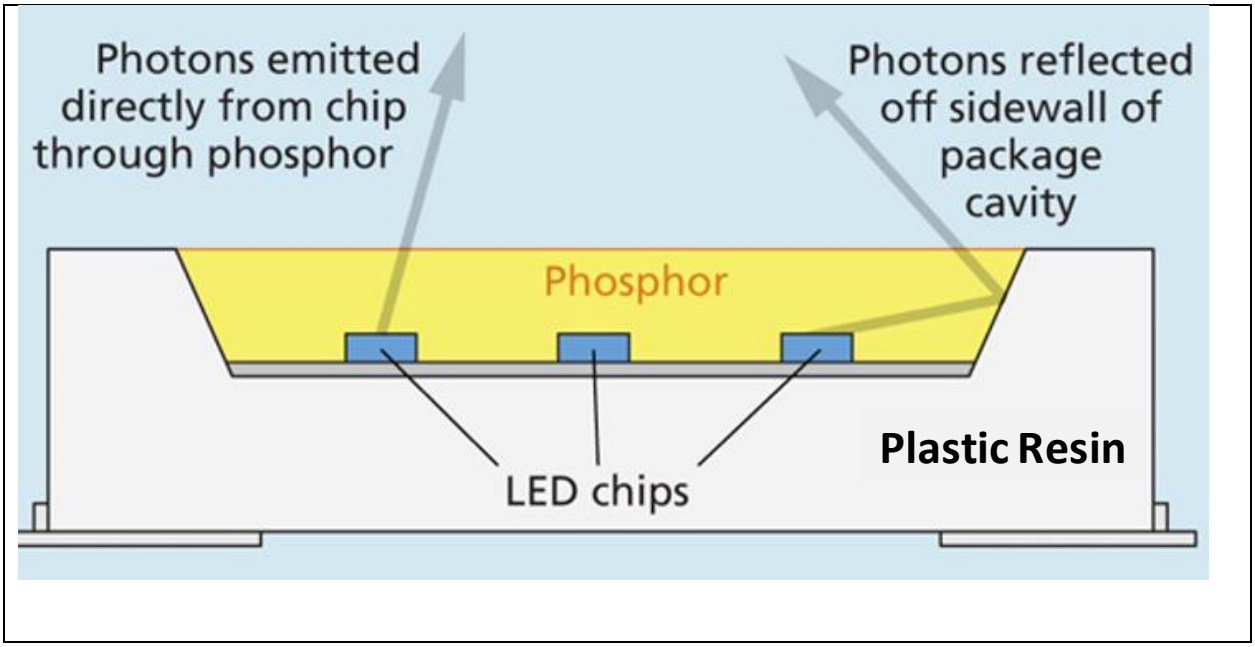

Figure 5-2. Simplified cross-section of a MP-LED package [13].

Likewise, package effects could have impacted the horticulture lamps examined in this study if the reflectance of the MP-LED sidewalls degraded over time. The MP-LEDs used in the MULTI-H1 product contain pcLEDs that use a blue die (approximately 453-nm peak wavelength) and a phosphor with a peak emission near 664 nm. If the reflectance from the package sidewall was reduced due to increased light absorption by the sidewalls of the LED package, then the chromaticity shift of the device would be expected to move toward the blue direction (i.e., $\Delta u'$ and $\Delta v'$ would both be negative). Instead, the chromaticity of the MULTI-H1 device shifted toward the red direction (i.e., $\Delta u'$ and $\Delta v'$ would both be positive) as shown in Figure 4-7, due to blue light absorption from the lens. Because lens absorbance was so dominant, the impact of polymer degradation in the LED package could not be determined by the time the experiment was terminated. The LEDs used in this device had a high level of phosphor loading, so it is likely that phosphor conversion reduced the amount of blue photons hitting the sidewalls of this package and lessened interior degradation of the polymer in the LED package, which would enable the lens yellowing mechanism to dominate the chromaticity and luminous flux maintenance.

Based on these findings, the package effects in MP-LEDs can significantly affect the parametric reliability of multi-source LEDs. The probability of this failure mode occurring is higher for LEDs with cooler CCTs (due to the higher blue light content) and lower for LEDs with a higher percentage of phosphor conversion.

The Impact of the Secondary Lens

The secondary lenses used in SSL devices are lenses external to the LED package that provide protection of the interior components (e.g., LEDs, electronics) from environmental elements (e.g., temperature, humidity). Good protection is especially important in horticulture and outdoor lighting applications because SSL devices can encounter a wide range of environmental stressors and other adverse conditions (e.g., dust, chemicals). A variety of polymer resins, including polymethyl methacrylate (PMMA), silicones, PC, and glasses, are used as secondary lenses for SSL devices [11, 24]. Of the common materials used for lenses, PC lenses are the most likely to discolor; this discoloration occurs with exposure to elevated temperatures, humidity, and blue photon flux [24]. The discoloration of PC generally proceeds as increased absorption of light, and this effect is especially pronounced at wavelengths below 500 nm, producing a yellow color in the lens [10, 24, 25].

During this study, both of the horticulture products contained PC lenses, but they represent two different ways in which lenses are used in SSL products. For the MULTI-H2 product, each LED has a separate lens molded into the overall lens assembly, and blue light and red light passed through individual lenses, thereby enabling a comparison of the degradation of lens irradiated by the two different LEDs. For the MULTI-H1 product, most of the light passed through the central concave lens, which is slightly larger than the LED array, thereby allowing a comparison of light emissions at different flux levels across the lens.

As shown in Figure 4-5, the initial radiant flux of blue light in the MULTI-H2 DUTs was 0.8 W, whereas the initial radiant flux of the red emissions was 2.1 W. Despite the lower radiant flux, the lenses over the LEDs with blue emissions discolored to a much greater extent than that observed over the red LEDs (see Figure 4-11), and the transmittance of the lenses over the blue LEDs was significantly lower after 8,000 hrs of 6590 exposure than the transmittance of lenses over the red LEDs (see Figure 4-13). The net result of the discoloration of the lens was an attenuation of blue emissions and a significant shift in the peak wavelength for blue emissions.

For the MULTI-H1 DUTs, the initial radiant flux of the blue emissions was also 0.8 W, whereas the initial radiant flux from the far-red phosphor produced 3.4 W of radiation (see Figure 4-3). The LED modules used in these DUTs were in the center of the lamp, directly underneath the central concave lens. Although blue light emissions were observed across this lens, the photon flux was significantly higher for the central concave lens than in the periphery of the combined lens. As a result, the central portion of the lens is strongly discolored, whereas the periphery is much less discolored (see Figure 4-10). Therefore, although the lens experienced the same temperature and humidity levels across its surface, the difference in photon flux between the center and periphery of the lens resulted in significant discoloration. The net result of the attenuation of the blue emissions by the lens was a chromaticity shift toward the red direction.

Because every photon produced by an SSL device passes through a secondary lens (if present) before illuminating a space, lens discoloration can have significant implications for outdoor, horticulture, and other specialty applications, as shown by this study. The impact of high blue photon flux must be considered when designing a lighting product to ensure high reliability against parametric failure (e.g., luminous flux, chromaticity). This reliability against a parametric failure is especially true if there is a significant spectral difference for different sections of the lens, if there is a significant radiant flux distribution across the lens, or if there is a variation in thickness across the lens [27].

For horticulture and outdoor lighting, the probability of lens discoloration is high if the lens is made with PC, but it is much lower if other resins such as PMMA or silicone are used. The probability for PC discoloration is especially high if heat, humidity, and blue light are present. For indoor lighting, the impact of lens

discoloration is expected to be low because temperature and humidity levels are generally controlled in buildings.

The Impact of Secondary Reflectors and Housings

In a similar manner, discoloration of reflective surfaces within an SSL device (e.g., optical mixing cavities, solder mask over LED modules, housings) can impact the luminous flux and chromaticity maintenance in SSL devices. The solder mask on all of the devices examined in this study discolored during testing, and as shown in Figure 3-2, this discoloration had a disproportional impact on wavelengths less than 550 nm. A similar effect was observed for the PC reflector in the MULTI-H1 DUTs in this study, as well as on paints used in SSL device housings in another study [25]. Therefore, the probability of reflector discoloration is high for some polymers (i.e., PC) especially if a photo-catalyst such as titanium dioxide is used as a pigment [25]. Fortunately, the impact of reflector discoloration on the optical performance of an SSL device is often much less than the impact of lens discoloration [10, 25]. As a result, reflector discoloration, including reflective assemblies and solder masks, is usually a minor contributor to the optical performance of a multi-source LED device.

The Impact of the Electronics and Controls

The architecture of a multi-source LED device can have a significant impact of the role of the electronics in device reliability, and the devices included in this report represent two different architectures for operating devices with multi-source LEDs. WTL and CTL require separate electrical control channels in the driver for each LED primary, and the reliability of select multi-channel drivers is reported in another publication [28]. If there is a failure in one of the independent driver channels powering WTL and CTL devices, then there will be significant impact on the chromaticity of the device and possibly the luminous flux maintenance [8]. However, the device will still produce light, but the quality of the light may be low. Both horticulture lamps examined in this study contain multi-source LED modules that are fed by a single direct current input. Consequently, if there is a failure in the driver circuit, then the device will go dark and experience an abrupt failure. In this architecture, there will be no period of low quality light as would occur with WTL and CTL systems.

6 Conclusions

The components and sub-components comprising SSL systems can degrade over time to change the parametric qualities of the device to the point where parametric failures occur. The occurrence of these parametric failure modes is especially critical in multi-source LED systems where differential changes in LED primaries and other system components can have a significant effect on light quality as summarized in **Table 6-1**. Because of their relatively complex architecture, multi-source LED devices present greater challenges in assessing the reliability and long-term device performance than do fixed-CCT products. Out of the parametric failure modes listed in **Table 6-1**, changes in phosphors, LED packages, and secondary optics are the most probable for multi-source LED devices and will likely have the largest impact on reliability. Understanding the impacts of multiple LED sources on an entire lighting system—especially the impacts of LED primaries that emit light at different wavelengths and respond to stressors encountered during use (e.g., heat, humidity) in vastly different ways—is critical to understanding the long-term reliability of such devices. This information is also critical to developing multi-source LED products with the lifetime and reliability needed to meet future lighting application needs.

Table 6-1. Sub-components of multi-source LED devices and the level of impact on device reliability.

Sub-component	Probability of Failure	Impact of Failure	Type of Failure	Comments
LED chip	Low	High	Predominantly parametric	Royal blue and red LEDs are generally stable, but other colors may show more drift with temperature and current.
Phosphors	High for warm white; low for cool white	High	Predominantly parametric	Warm white phosphors can be prone to chromaticity shifts in the green direction, and other phosphors can be more susceptible to quenching processes over time. Cool white phosphors (e.g., YAG:Ce) are generally more stable.
LED package	High for cool white, and low for LEDs with high phosphor loadings (e.g., warm white, red)	High	Predominantly parametric	The level of blue irradiation in the package impacts photo-oxidation of polymer resins used in its construction. MP-LEDs operating at cool CCT values are more susceptible to package-induced chromaticity and luminous flux effects due to the higher blue light content. MP-LEDs with more phosphor conversion of the blue light have lower package effects to adversely impact luminous flux and chromaticity.
Secondary lenses	High for PC, especially in the presence of heat and humidity; low for PMMA, silicone, and glass	High	Predominantly parametric	Discoloration of secondary optics can have a significant impact on parametric failure. The lens tend to increase in blue-light absorption over time, and the effect is promoted by temperature, humidity, and blue irradiation. Spatial variability in blue irradiation will cause selective yellowing in areas of the lens with high radiant flux.
Secondary reflectors	High for some polymers (e.g., PC), but lower for some paints and expanded foam diffuse reflectors [25]	Low	Predominantly parametric	Secondary reflectors, solder masks, and housings made with polymers can also undergo discoloration whenever temperature, humidity, and blue light irradiation are present. The relative impact is dependent on the design of the SSL device with deeper optical mixing cavities, leading to a greater negative impact for discolored reflector surfaces.

Sub-component	Probability of Failure	Impact of Failure	Type of Failure	Comments
Electronics	Moderate	Moderate	Abrupt failure or parametric failure	Impacts vary widely depending on system design. For WTL devices, a failure of the electronics driving one LED primary can affect light quality, but the device still produces light even when it is in a partially failed state. For multi-source LEDs containing a single input voltage to the LED module, driver failure results in a complete "lights out" failure.

7 References

1. Davis, J. L. (2018, May). *Luminaires for advanced lighting in education*. Presented at LightFair International 2018, Chicago, IL.

2. Wilkerson, A., Davis, R. G., & Clark, E. (2017, August). *Tuning hospital lighting: Evaluating tunable LED lighting at the Swedish Hospital Behavioral Health Unit in Seattle*. Report PNNL-26606. Prepared for the U.S. Department of Energy Solid-State Lighting Program. Available at https://www.energy.gov/sites/prod/files/2017/08/f36/2017_gateway_swedish-tuning-led_0.pdf

3. Pacific Northwest National Laboratory. (2018, August). *CALiPER report 23: Photometric testing of white-tunable LED luminaires*. Prepared for the U.S. Department of Energy Solid-State Lighting Program. Available at https://www.energy.gov/sites/prod/files/2018/09/f55/caliper_23_white-tunable-led-luminaires_0.pdf

4. Lucas, R. J., Peirson, S., Berson, D. M., Brown, T. M., Cooper, H. M., Czeisler, C. A., et al. (2014). Measuring and using light in the melanopsin age. *Trends in Neurosciences, 37*(1), 1–9.

5. Paolini, S. (2018). *R&D directions in color tunable lighting.* Presented at the 2018 U.S. Department of Energy Solid-State Lighting Program Research and Development Workshop, Nashville, TN. Available at https://www.energy.gov/sites/prod/files/2018/02/f48/paolini_directions_nashville18_1.pdf

6. Mitchell, C. A., Dzakovich, M. P., Gomez, C., Lopez, R., Burr, J. F., Hernandez, R., et al. (2015) Light-emitting diodes in horticulture. *Horticulture Reviews, 43*. doi: 10.1002/92781119107781.ch01

7. Next Generation Lighting Industry Alliance and LED Systems Reliability Consortium. (2014, September). LED luminaire lifetime: Recommendations for testing and reporting. 3rd Edition. Available at https://www.energy.gov/sites/prod/files/2015/01/f19/led_luminaire_lifetime_guide_sept2014.pdf

8. Davis, J. L., Rountree, K. J., & Mills, K. C. (2018, March). *Accelerated stress testing of multi-source LED Products: Horticulture lamps and tunable-white modules.* Prepared for the U.S. Department of Energy. Available at https://www.energy.gov/sites/prod/files/2018/05/f51/ssl_ast-multi-source-led_2018.pdf

9. Hansen, M. (2015). *The true value of LED packages*. Presented at the 2015 Strategies in Light Conference, Las Vegas, NV.

10. International Commission on Illumination. (1998). CIE 130-1998: Technical report on practical methods for the measurement of reflectance and transmittance. Vienna, Austria.

11. Davis, J. L., Mill, K., Lamvik, M., Solano, E., Bobashev, G., & Perkins, C. (2017). *Modeling the impact of thermal effects on luminous flux maintenance for SSL luminaires*. Presented at the 2017 16th IEEE Intersociety Conference on Thermal and Thermomechanical Phenomena in Electronic Systems (ITherm), Orlando, FL. doi: 10.1109/ITHERM.2017.7992598

12. Davis, J. L., Mills, K., Yaga, R., Johnson, C., Hansen, M., & Royer, M. (2018). Chromaticity maintenance in LED devices. In Van Driel, W., Fan, X., & Zhang, G. (eds.). Solid State Lighting Reliability Part 2: Components to Systems. Springer.

13. Tuttle, R., & McClear, M. (2014). Understanding the true cost of LED choices in SSL systems. *LEDs Magazine*. Available at https://www.ledsmagazine.com/leds-ssl-design/packaged-leds/article/16695263/understand-the-true-cost-of-led-choices-in-ssl-systems-magazine

14. Tsai, M.-Y., Tang, C.-Y., Wang, C. J., Tsai, Y. Y., & Chen, C.-H. (2015). Investigation on some parameters affecting optical degradation of LED packages during high-temperature aging. *IEEE Transactions on Device and Materials Reliability, 15*(3), 335–341.

15. Lu, G, van Driel, W. D., Fan, X., Yazdan Mehr, M., Fan, J., Jansen, K. M. B., et al. (2015). Degradation of microcellular PET reflective materials used in LED-based products. *Optical Materials, 49*, 79–84. doi: 10.1016/j.optmat.2015.07.026

16. Osram Opto Semiconductors. (2011, May). Reliability of the DRAGON product family: Application note. Available at https://dammedia.osram.info/media/resource/hires/osram-dam-2496619/Reliability%20of%20the%20DRAGON%20Product%20Family.pdf

17. Bobashev, G., Baldasaro, N. G., Mills, K. C., & Davis, J. L. (2016). An efficiency-decay model for lumen maintenance. *IEEE Transactions on Device and Materials Reliability, 16*(3), 277–281.

18. IES (Illuminating Engineering Society). (2011). IES TM-21-11: Projecting long term lumen maintenance of LED light sources. Illuminating Engineering Society, New York, NY.

19. Tu, P. L., Chan, Y. C., & Lai, J. K. L. (1997). Effect of intermetallic compounds on the thermal fatigue of surface mount solder joints. *IEEE Transactions on Components, Packaging, and Manufacturing Technology—Part B, 20*(1), 87–93.

20. Yeh, C.-W., Chen, W.-T., Liu, R.-S., Hu, S.-F., Sheu, H.-S., Chen, J.-M., et al. (2012). Origin of thermal degradation of $Sr_{(2-x)}Si_5N_8:Eu_{(x)}$ phosphors in air for light-emitting diodes. *Journal of the American Chemical Society, 134*(34), 14108–14117.

21. Davis, J. L., Mills, K. C., Bobashev, G., Rountree, K. J., Lamvik, M, Yaga, R., et al. (2018, May). Understanding chromaticity shifts in LED devices through analytical models. *Microelectronics Reliability, 84*, 149–156. doi: https://doi.org/10.1016/j.microrel.2018.03.023

22. Davis, J. L., Young. J., & Royer M. A. (2016, February). *CALiPER Report 20.5: Chromaticity shift modes of LED PAR38 lamps operated in steady-state conditions.* Prepared for the U.S. Department of Energy Solid-State Lighting Program. Available at https://www.energy.gov/sites/prod/files/2016/03/f30/caliper_20-5_par38.pdf

23. Savin, N. E., & White, K. J. (1977, November). *The Durbin–Watson test for serial correlation with extreme sample sizes or many regressors*. *Econometrica, 45*(8), 1989–1996.

24. Yazdan Mehr, M., Bahrami, A., van Driel, W. D., Fan, X. J., Davis, J. L., & Zhang, G.Q. (2019, January). Degradation of optical materials in solid-state lighting systems. *International Materials Reviews*, 1-27. doi: https://doi.org/10.1080/09506608.2019.1565716

25. Davis, J. L., Mills, K. C., Johnson, C., Yaga, R., Bobashev, G., Baldasaro, N., et al. (2017, May 31). Final report: *System reliability model for solid-state lighting (SSL) luminaires*. Contract DE-EE0005124. Prepared for the U.S. Department of Energy Solid-State Lighting Program. Available at https://www.osti.gov/servlets/purl/1360770

26. Davis, J. L., Rountree, K., & Mills, K. C. (2018, July). Luminous flux and chromaticity maintenance for select high-power color light-emitting diodes. Prepared for the U.S. Department of Energy Solid-State Lighting Program. Available at https://www.energy.gov/sites/prod/files/2019/01/f58/ssl_rti_lm80-color-leds_july2018.pdf

27. Gandhi, H., Hein, C.L., van Heerbek, R., & Pickett, J.E. (2019). Acceleration parameters for polycarbonate under blue LED photo-thermal aging conditions. *Polymer Degradation and Stability*, 164, 69-74. https://doi.org/10.1016/j.polymdegradstab.2019.04.001

28. Davis, J. L., & Rountree, K. (2019). Accelerated stress testing results on single-channel and multichannel drivers: Final report. Prepared for the U.S. Department of Energy Solid-State Lighting Program.

Appendix 1—Chromaticity Shifts of MULTI-TW1 Light-Emitting Diode (LED) Modules

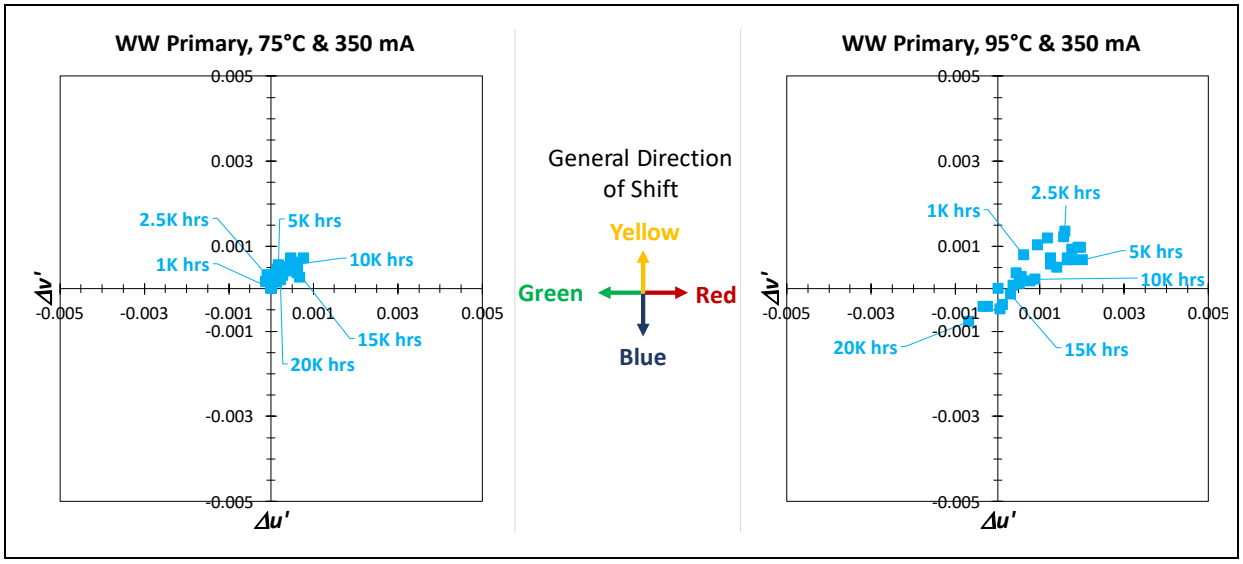

Figure A1-1. Chromaticity shifts for warm white (WW) primaries operated at 350 mA in 75°C temperature conditions (left) and 350 mA in 95°C temperature conditions (right).

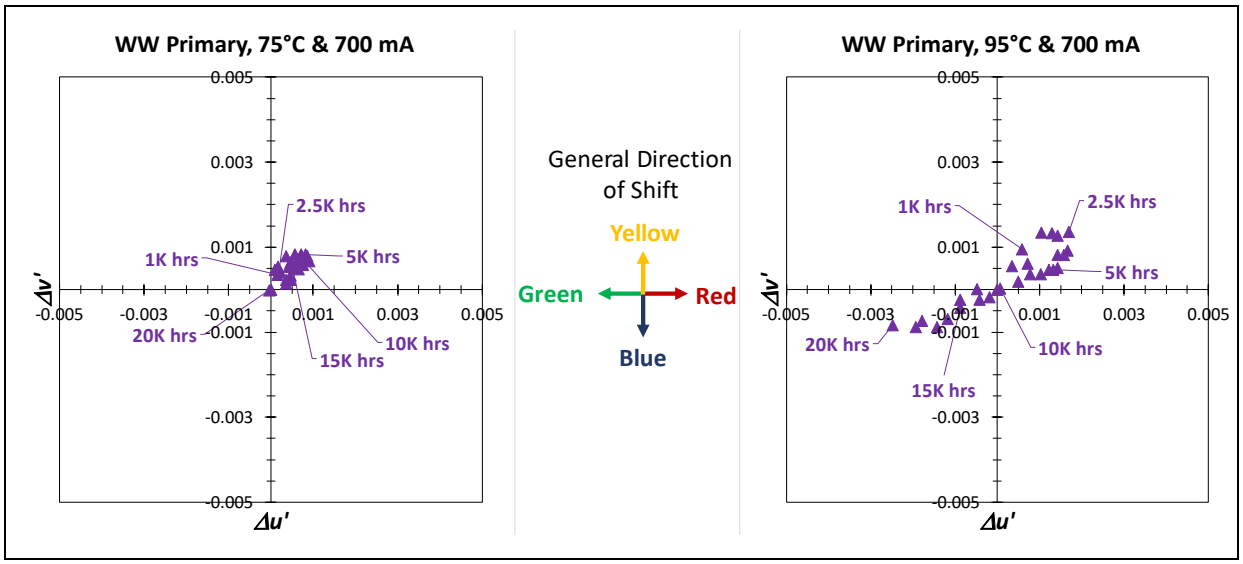

Figure A1-2. Chromaticity shifts for warm white (WW) primaries operated at 700 mA in 75°C temperature conditions (left) and 700 mA in 95°C temperature conditions (right).

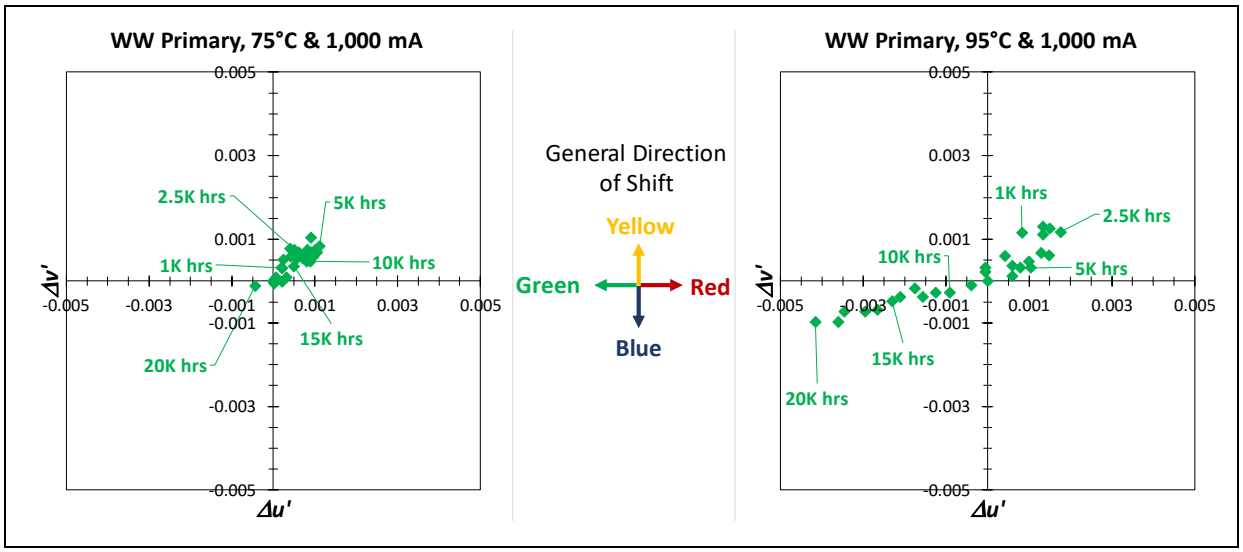

Figure A1-3. Chromaticity shifts for warm white (WW) primaries operated at 1,000 mA in 75 °C temperature conditions (left) and 1,000 mA in 95 °C temperature conditions (right).

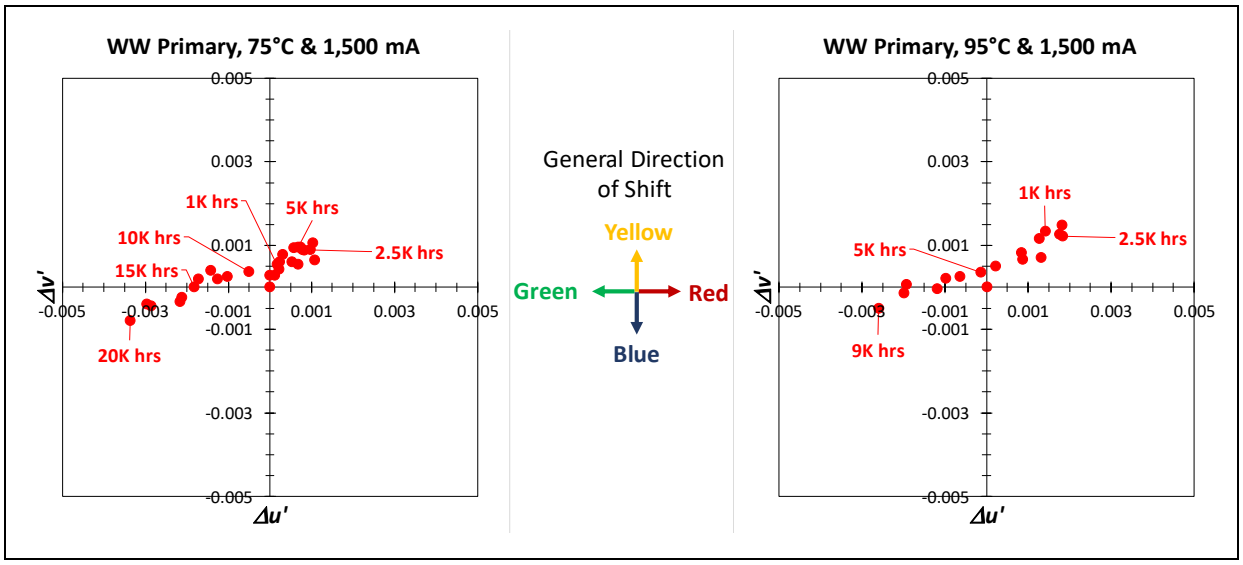

Figure A1-4. Chromaticity shifts for warm white (WW) primaries operated at 1,500 mA in 75 °C temperature conditions (left) and 1,500 mA in 95 °C temperature conditions (right).

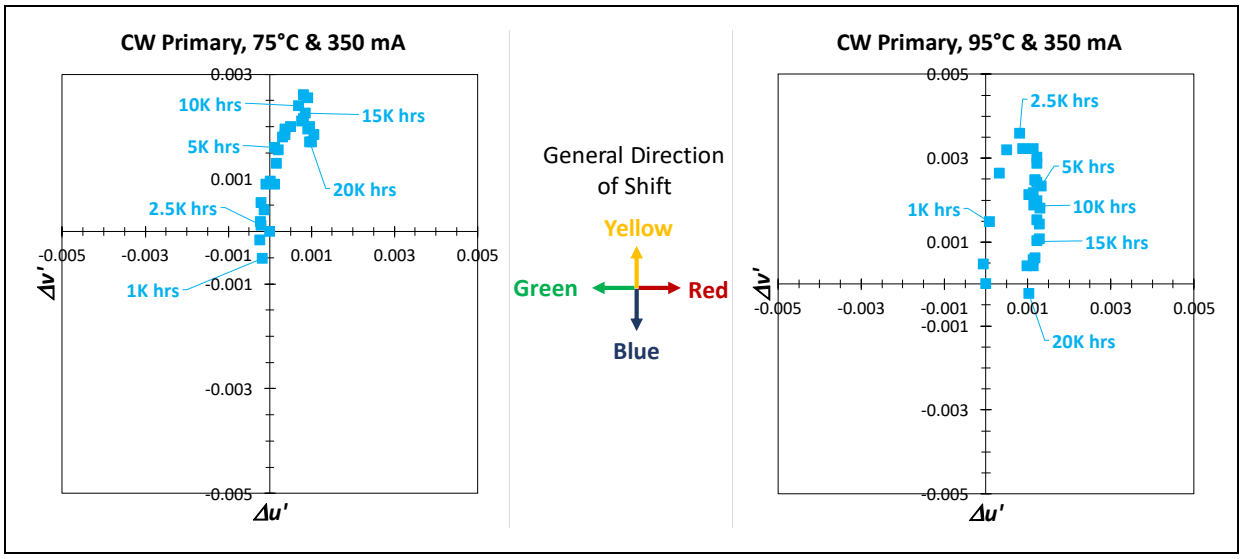

Figure A1-5. Chromaticity shifts for cool white (CW) primaries operated at 350 mA in 75 °C temperature conditions (left) and 350 mA in 95 °C temperature conditions (right).

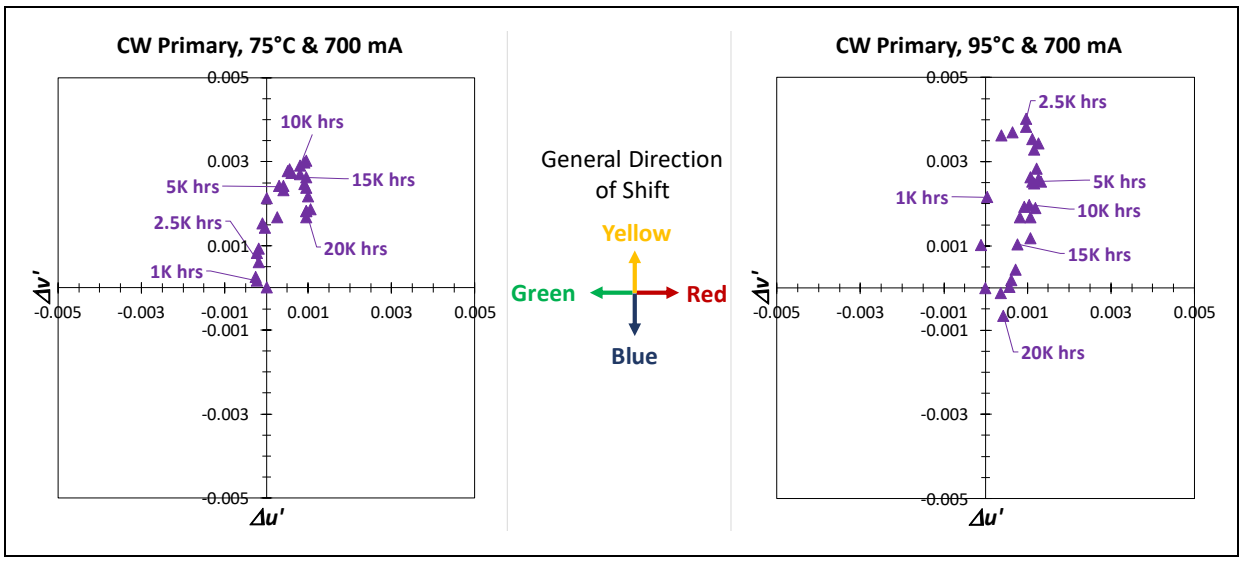

Figure A1-6. Chromaticity shifts for cool white (CW) primaries operated at 700 mA in 75 °C temperature conditions (left) and 700 mA in 95 °C temperature conditions (right).

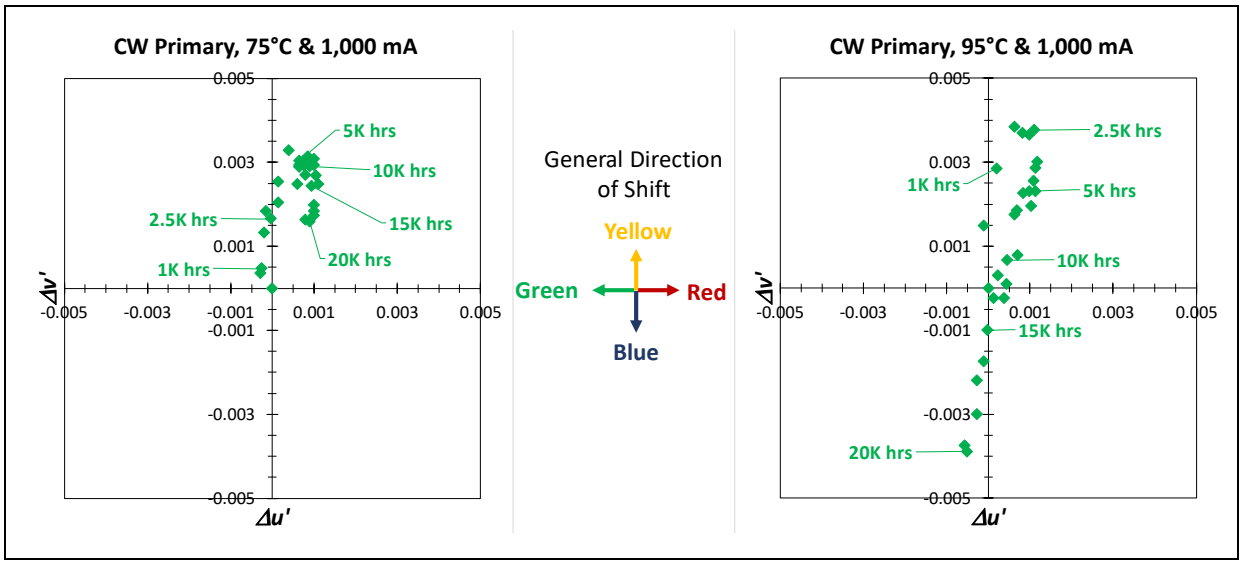

Figure A1-7. Chromaticity shifts for cool white (CW) primaries operated at 1,000 mA in 75°C temperature conditions (left) and 1,000 mA in 95°C temperature conditions (right).

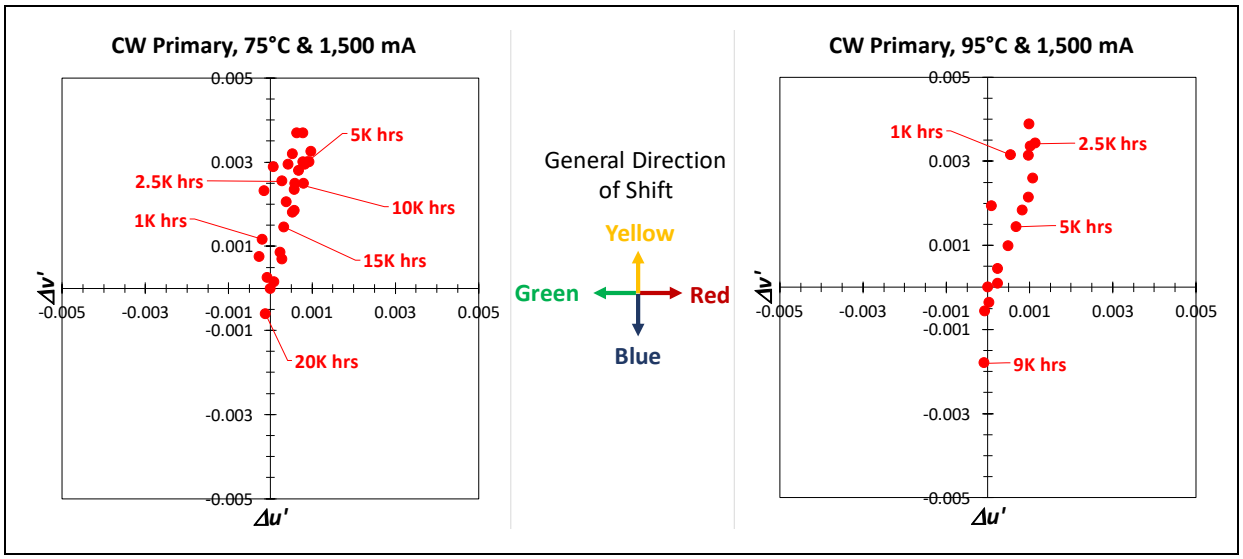

Figure A1-8. Chromaticity shifts for cool white (CW) primaries operated at 1,500 mA in 75°C temperature conditions (left) and 1,500 mA in 95°C temperature conditions (right).

U.S. DEPARTMENT OF
ENERGY

Office of
ENERGY EFFICIENCY &
RENEWABLE ENERGY

For more information, visit:
energy.gov/eere/ssl

DOE/EERE 1993 • July 2019